Advanced Workshop on Earthquake Fault Mechanics: Theory, Simulation and Observations
ICTP, Trieste, Sept 11 2019

Lecture 1: Array Seismology and MUSIC teleseismic Back-Projection

Lingsen Meng

UCLA Department of Earth, Planetary, and Space Sciences

Knopoff Chair

Big Thanks to:

Students & Postdocs:

Hui Huang

Chao An

Ailin Zhang

Han Bao

Yuqing Xie

Tian Feng

Tong Zhou

Zhipeng Liu

Collaborators:

Jean-Paul Ampuero

Yuji Yagi

Roland Burgmann

David Oglesby

Ryosuke Ando

Baoning Wu

Special thanks to:

The Knopoff family

Outlines

- Motivation: discover/validate complex rupture patterns
- Earthquake source imaging with back-projections (BP)
- Sensor array processing and direction of arrivals
- Beamforming
- Point spread function: evaluating resolution and aliasing
- MUltiple SIgnal Classification (MUSIC)
- Example 1: Encircling rupture of the 2015 Iallpel earthquake
- Example 2: Geometrical complexity of the 2012 Indian Ocean earthquake
- Example 3: Physical mechanisms of the 2013 Deep-focus Okhotsk earthquake

Complicated Rupture Patterns Emerge in Dynamic Simulations

The 2019 Mw 6.4 and Mw 7.1 Ridgecrest earthquake

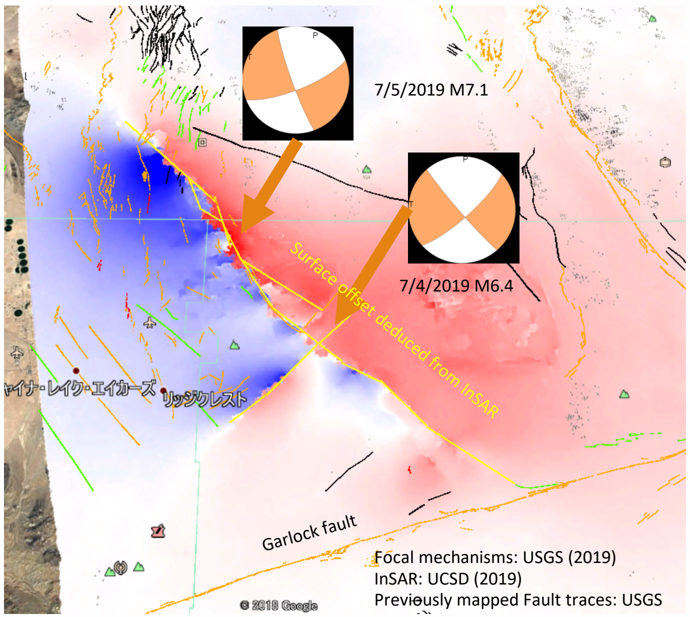

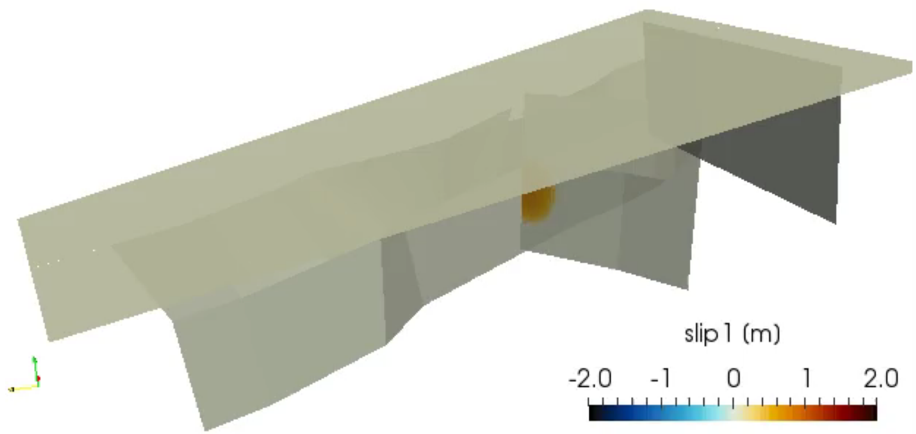

Credit: Ryosuke Ando

- Reproduce the pause of rupture at the both ends of foreshock area on the main fault

Complicated Rupture Patterns Emerge in Dynamic Simulations

The 2010 M 7.2 El Mayor Cupacah earthquake

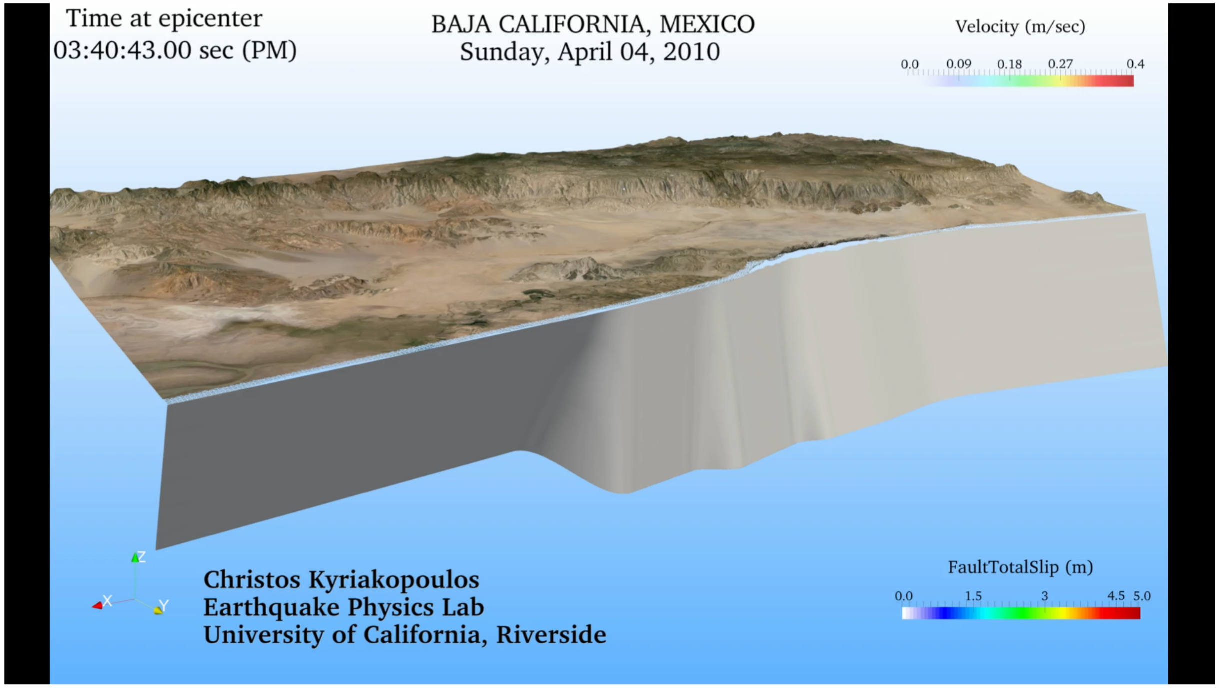

Kyriakopoulos et al., 2017

Hard to see in traditional source inversions based on seismic/geodetic observations (<1Hz)

Living in the Age Of Great Quakes

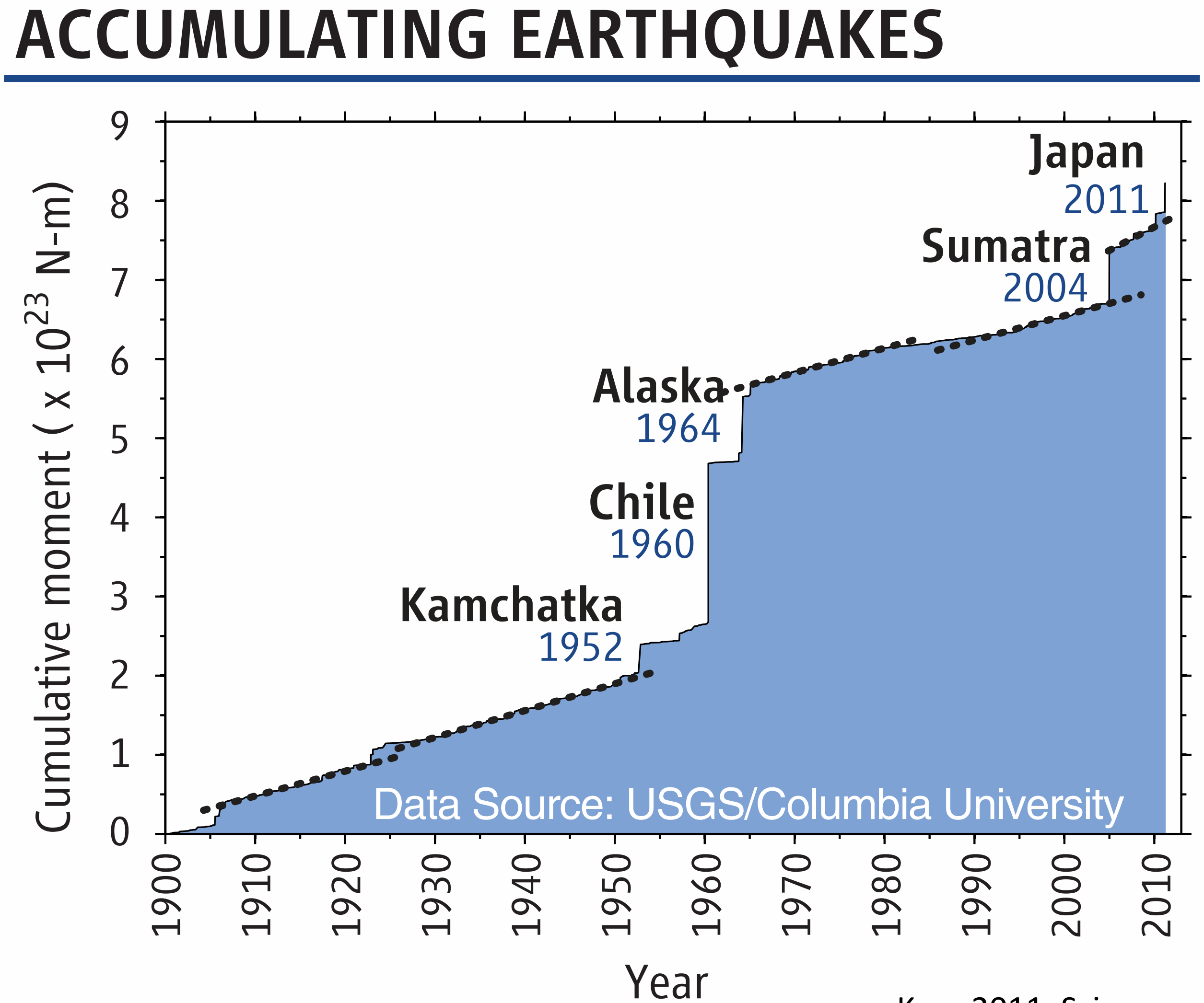

Kerr, 2011, Science

Finite Fault Models

A suite of models for the 1999 Izmit (Turkey, M 7.5)

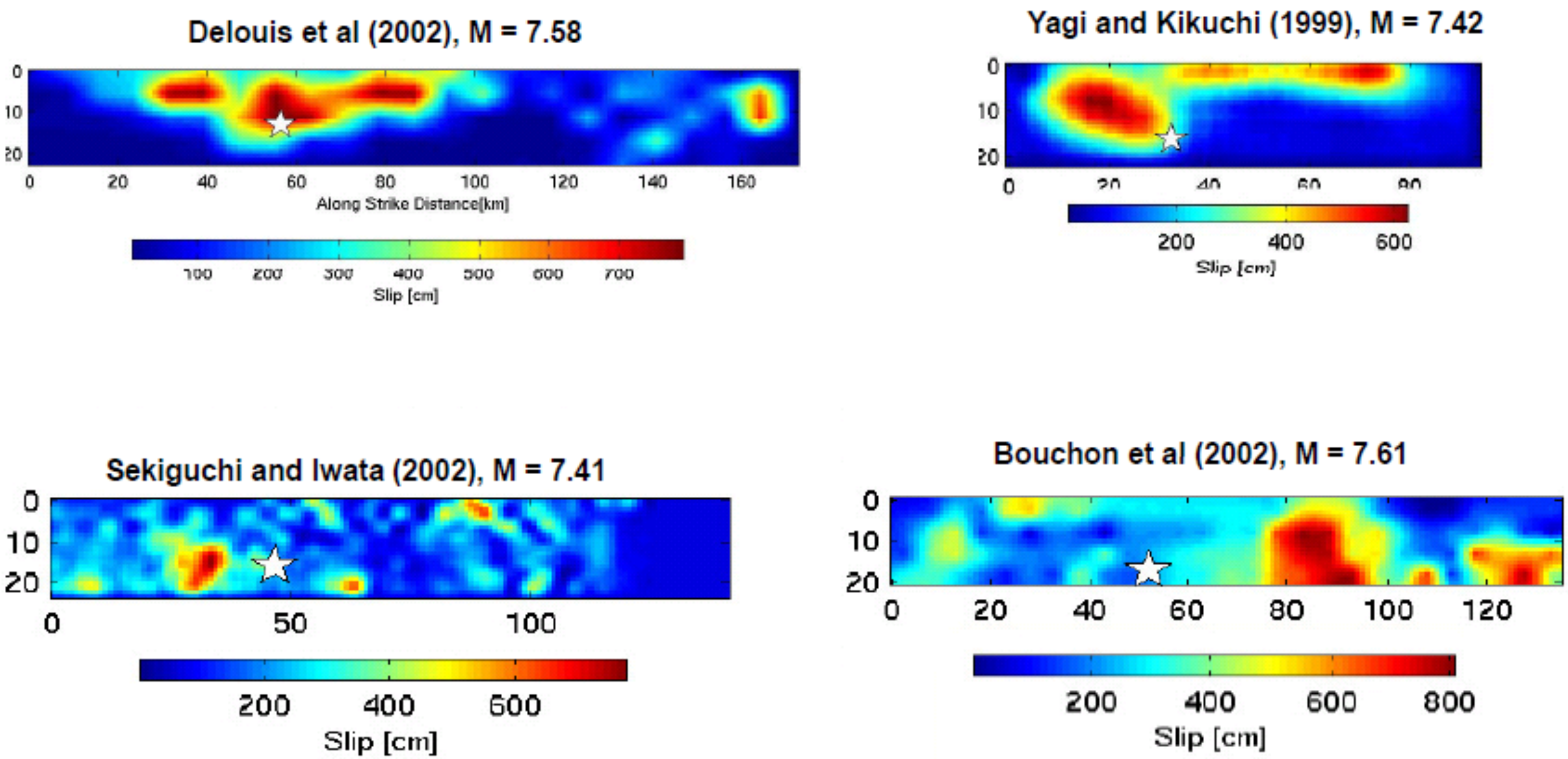

Back-Projection (BP)

Introduced by Ishii, Shearer et al (2005)

Advantage:

1. Based on body waves recorded at teleseismic distance by large seismic arrays
2. Capability to track areas of high-frequency energy radiation as the rupture grow
3. Requires fewer assumptions than traditional source inversion

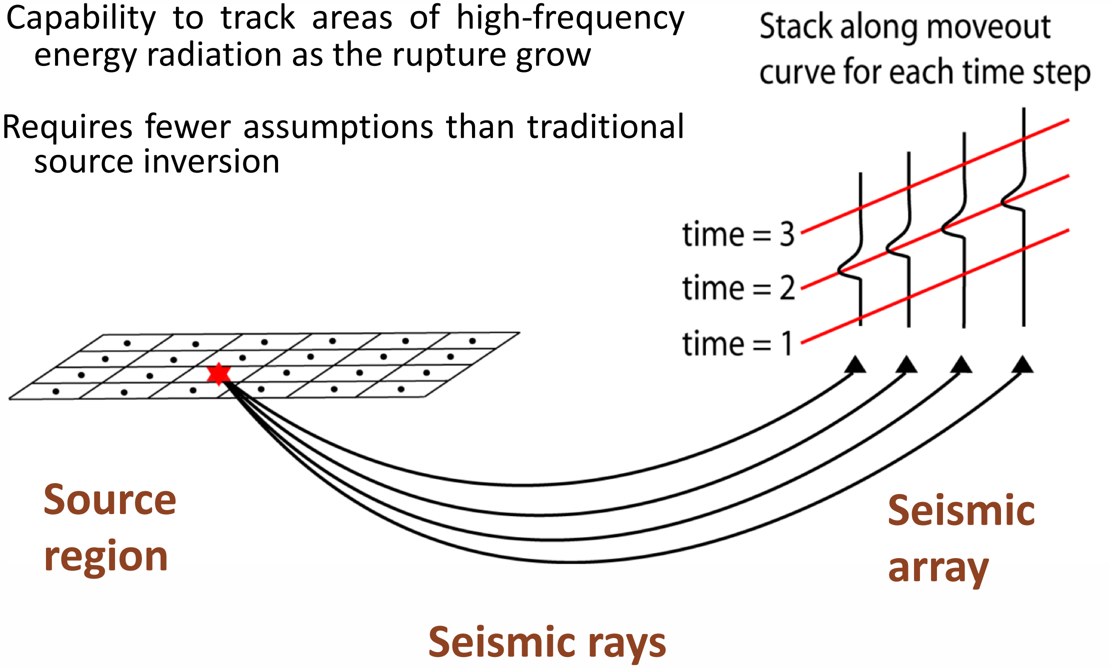

Tohoku Earthquake

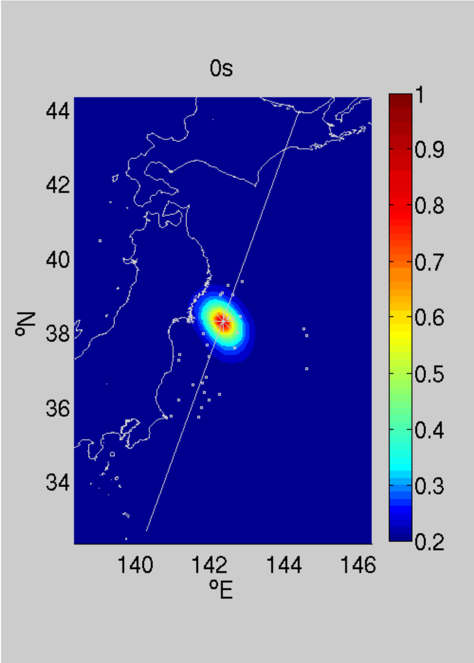

Meng et al., 2011

Anatomy of Back-projection Imaging

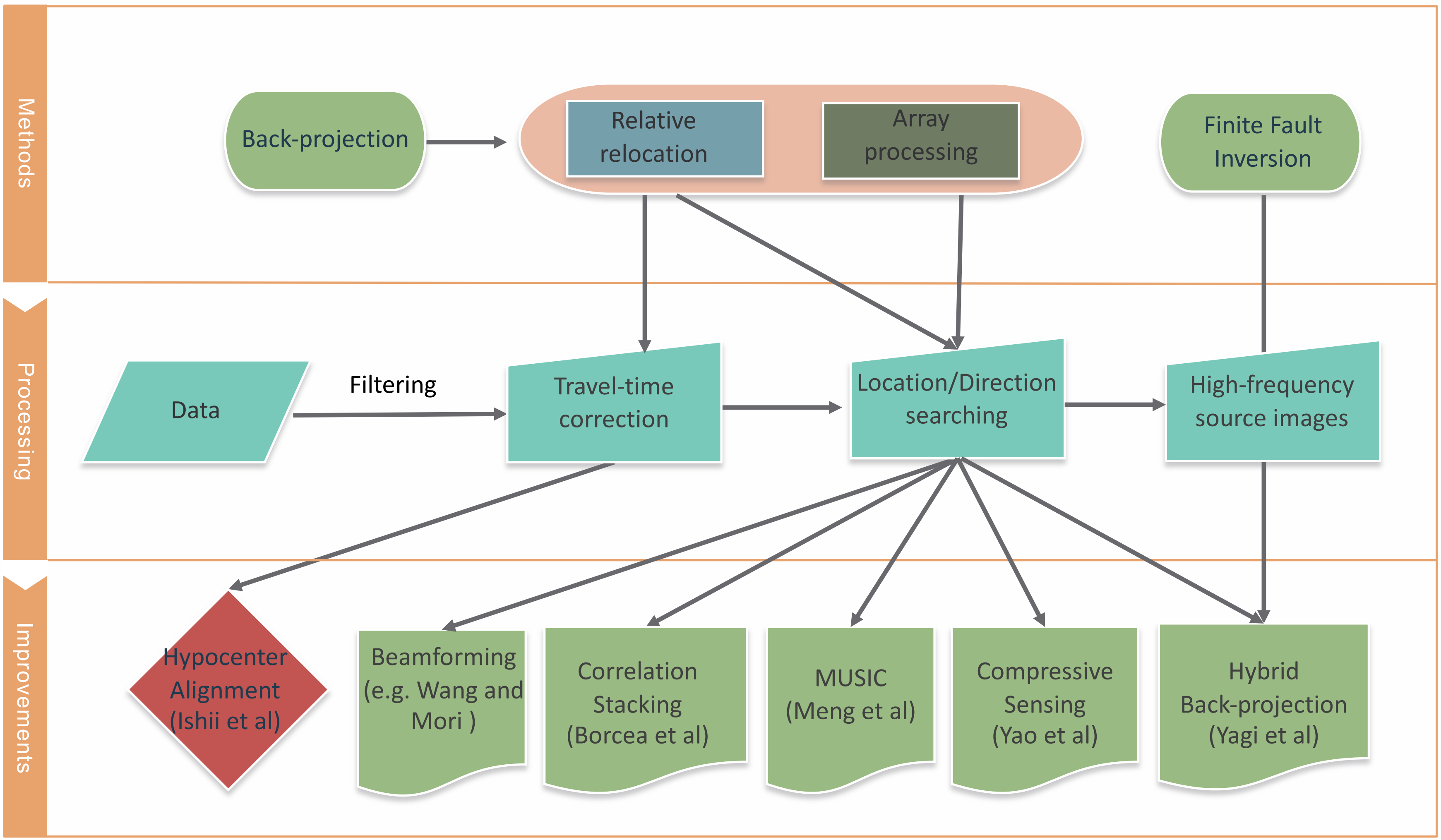

Improving Imaging Quality

Low Resolution High Resolution

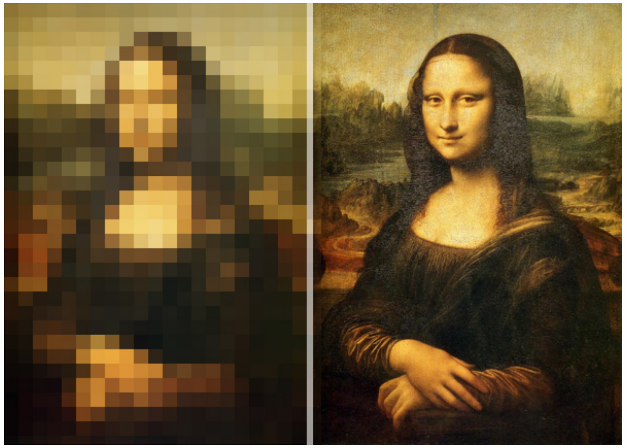

Low Accuracy High Accuracy

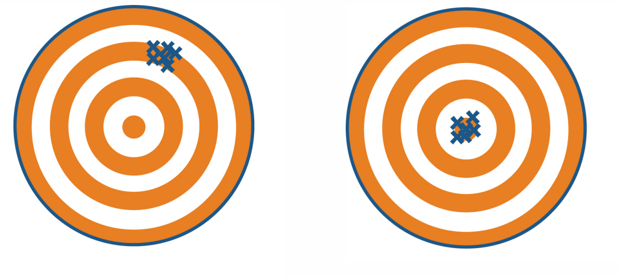

Objective: Improving Resolution
Solution: **MUSIC method**

Objective: Reduce Spatial Biases
Solution: **Slowness Calibration**

An example from daily life: sound localization

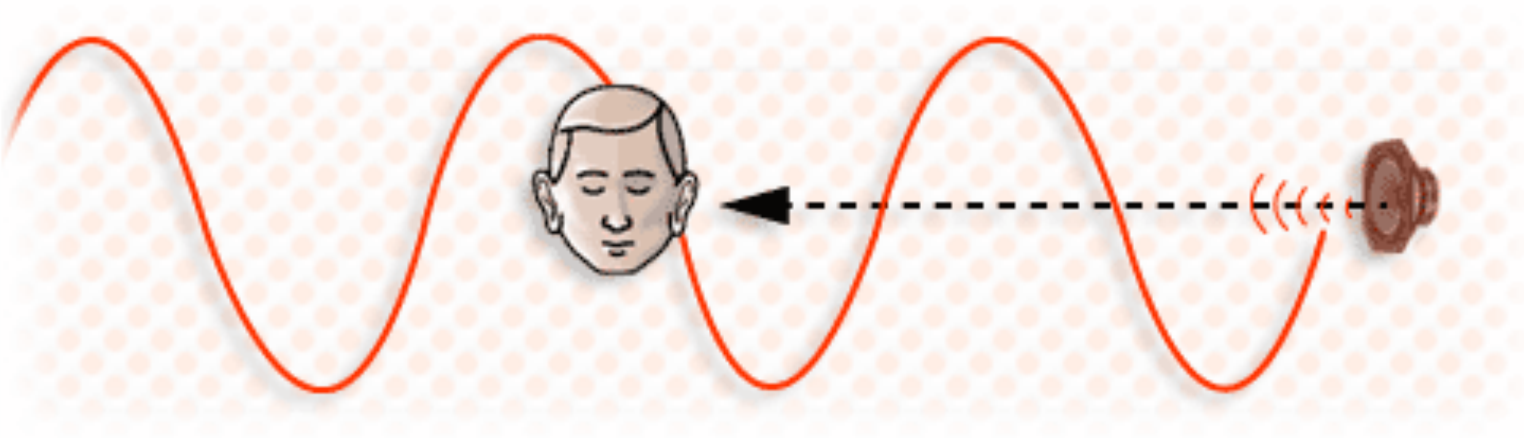

Our ears use the phase delay of sound to pinpoint the location of the source

This works also for a moving source

Sensor Array Processing

Communication

Sonar

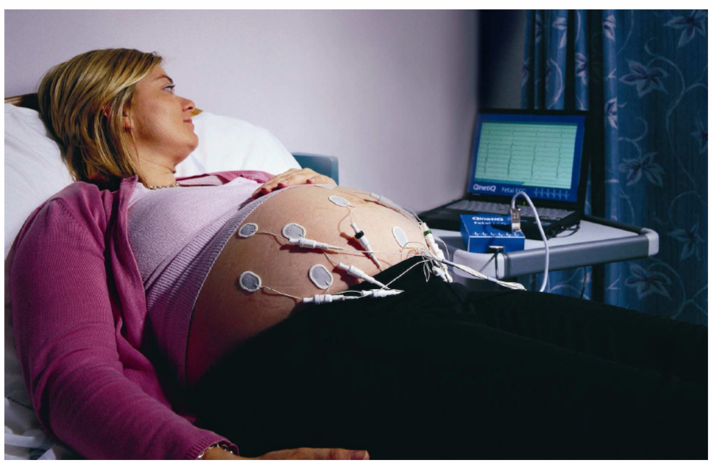

Biomedicine

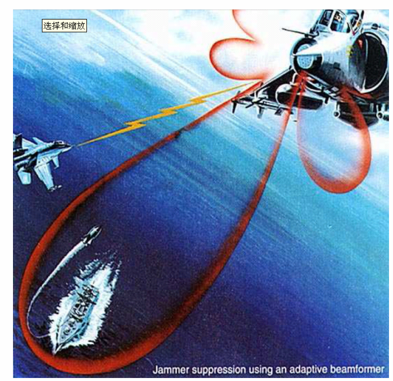

Radar

(Pictures from QinetiQ)

New Data from Large and Dense Arrays

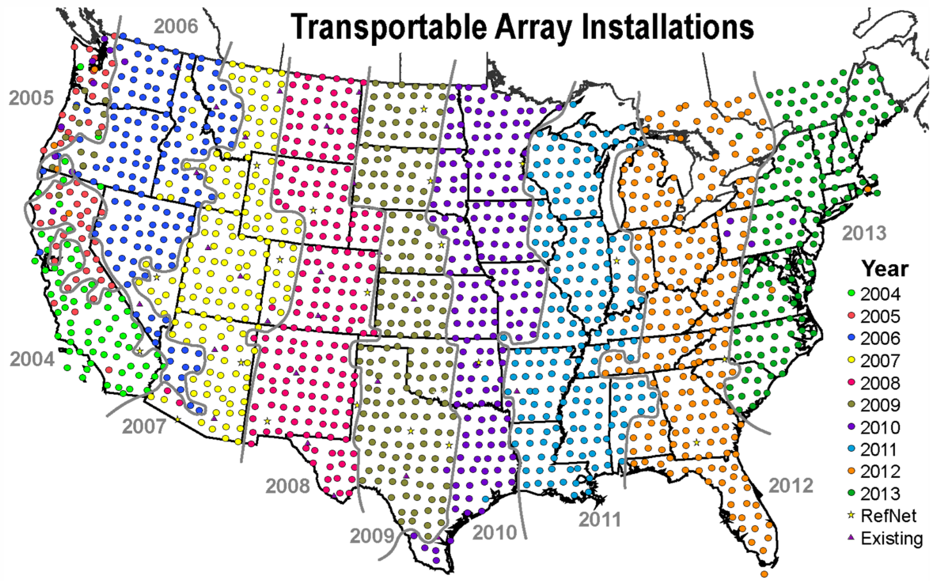

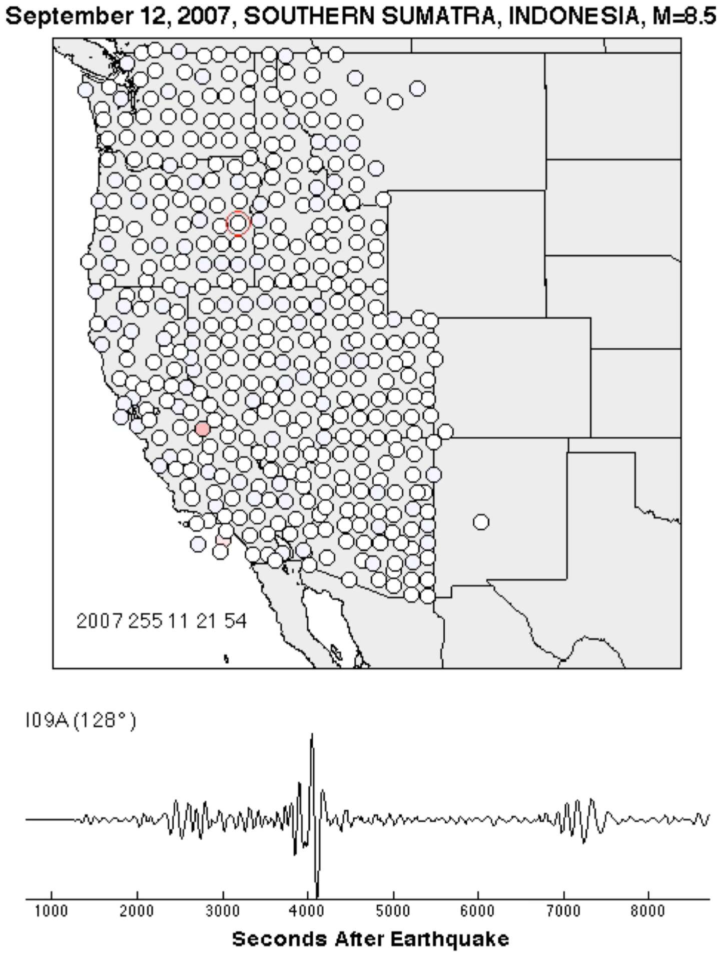

Teleseismic wavefield of large earthquakes recorded at an unprecedent level by USArray

Earthquake Source Imaging By Back-projection Of Array Data

The idea is to identify different arrival curves to recover source locations.

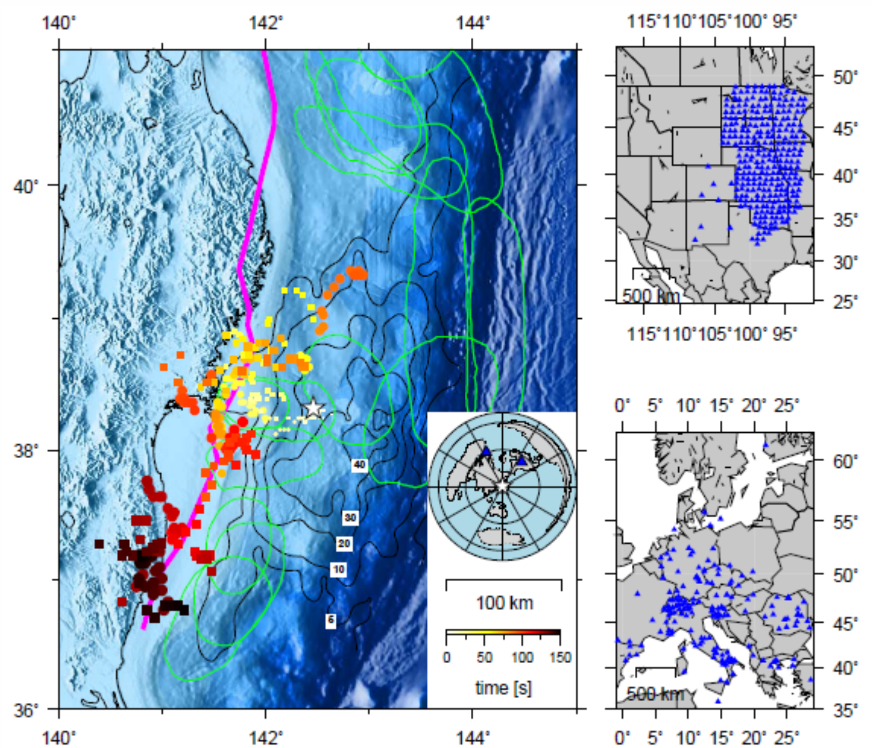

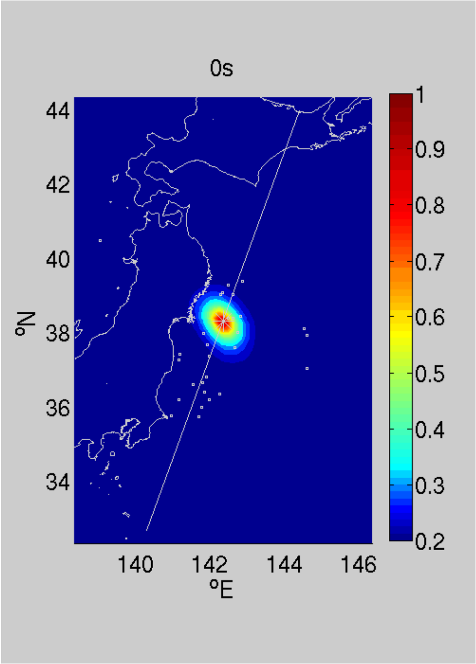

2011 Tohoku-Oki earthquake (Meng et al,2011)

Back-projection

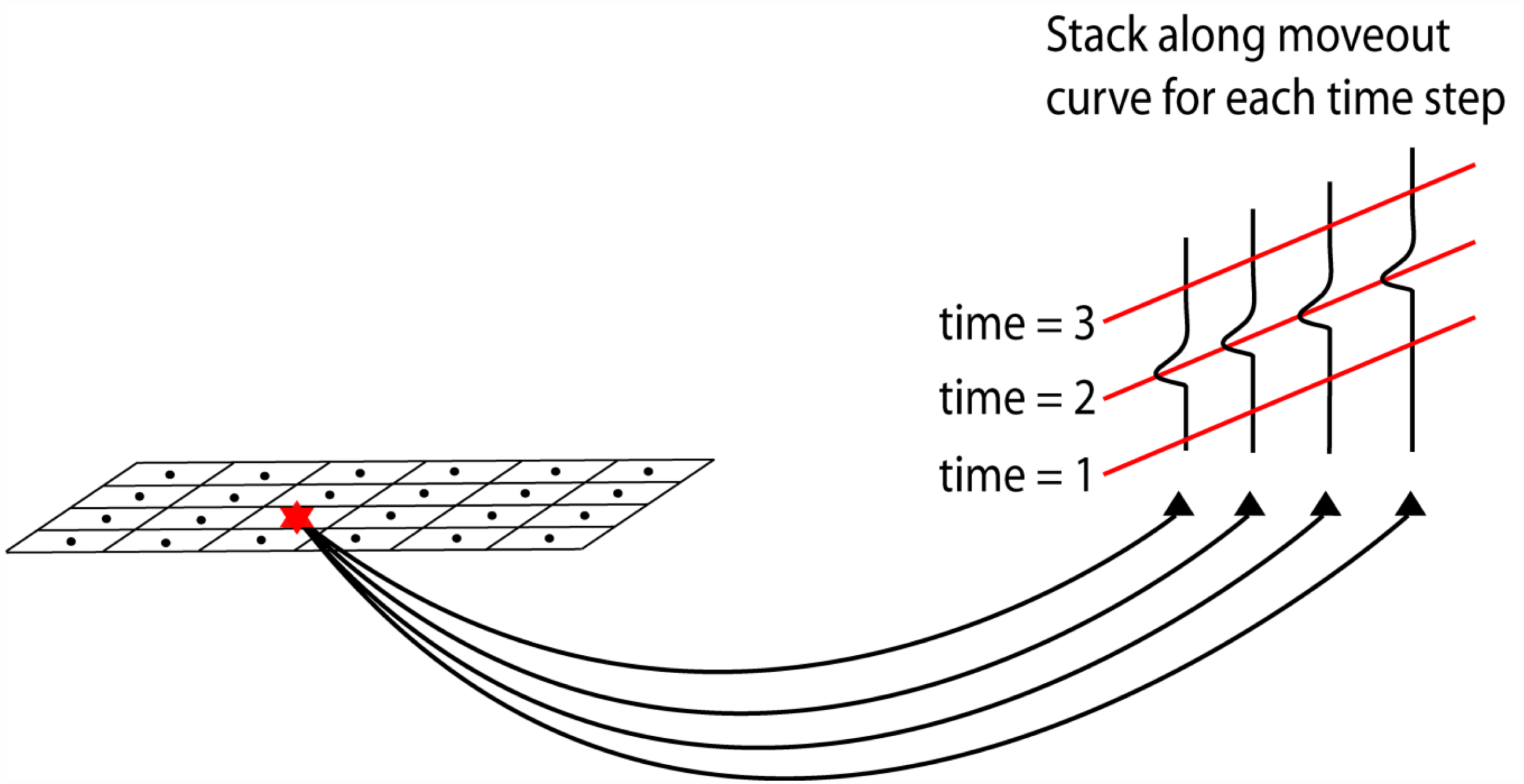

Beamforming

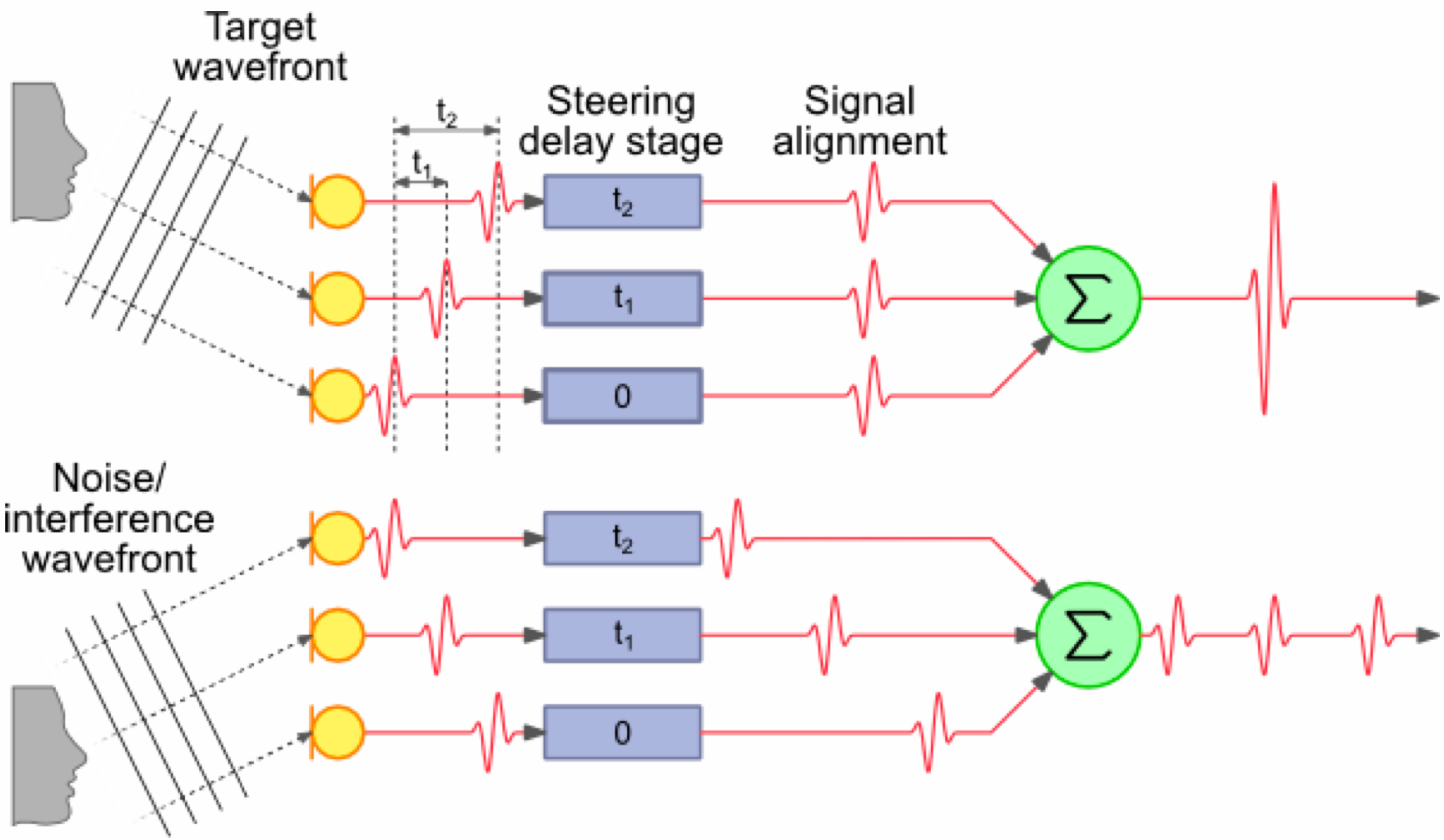

Credit: https://towardsdatascience.com

Beamforming (Delay and Sum)

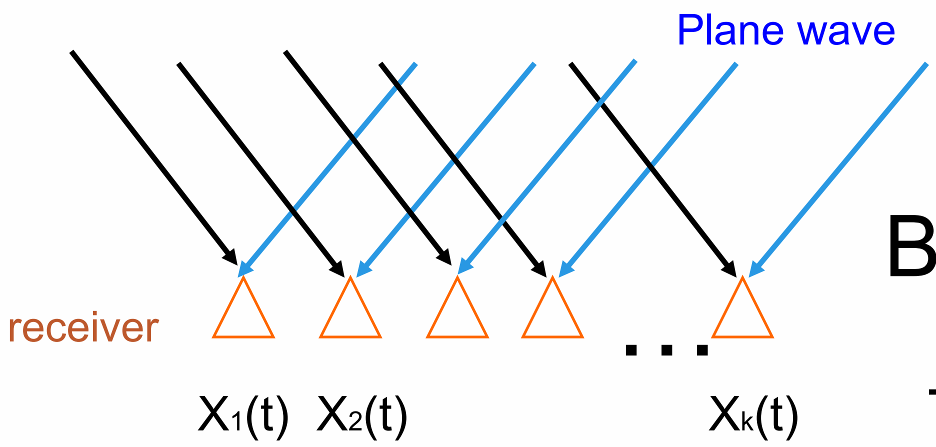

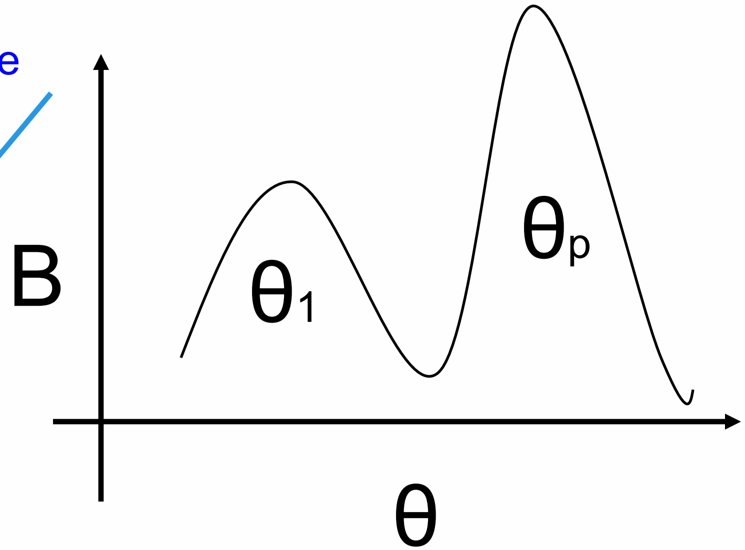

$$B(\theta) = \left\| \sum_k x_k(t + \tau_k(\theta, r_k)) \right\|$$

r, location of the sensor

Θ, direction of signal

τ, delay of the sensor

k, index of the sensor

Variants of Beamforming

$$B(\theta) = \int_t \left(\sum_k x_k(t + \tau_k(\theta, r_k))^{1/n} \right)^n$$

Nth root stacking

(e.g. Koper et al., 2011)

$$B(\theta) = \sum_i \sum_j C_{ij}(\tau_k(\theta, r_i, r_j))$$

Interferometic imaging

(correlation stacking)

(Frankel et al,1991

,Flechter & Spudich, 2006)

Rayleigh Criteria (resolution limit)

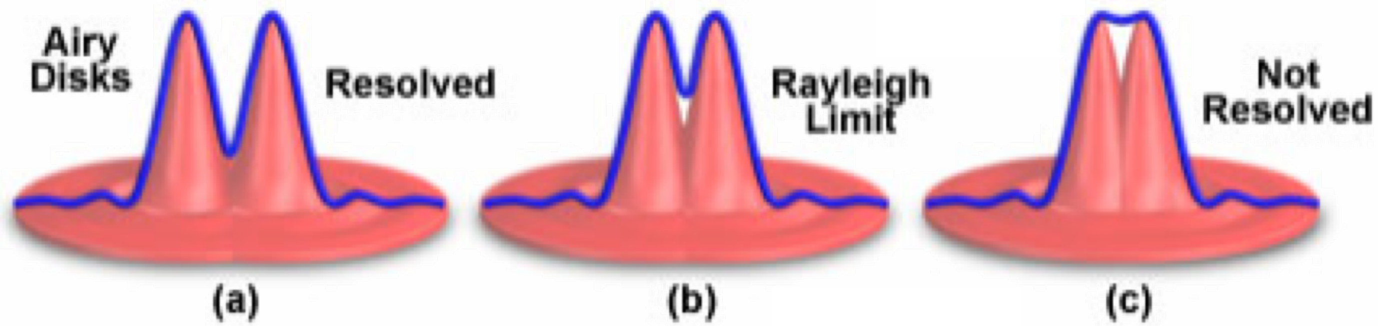

Rayleigh Criteria (resolution limit)

$$L \sim 1.22 \frac{\Delta \cdot \lambda}{A}$$

L, azimuthal resolution limit on the fault

Δ, distance away from the source

A, aperture of the array

λ, Horizontal wavelength

USArray Example : Δ=70° ,

λ=18 km/s*1s=18 km, A=25° , L=50 km

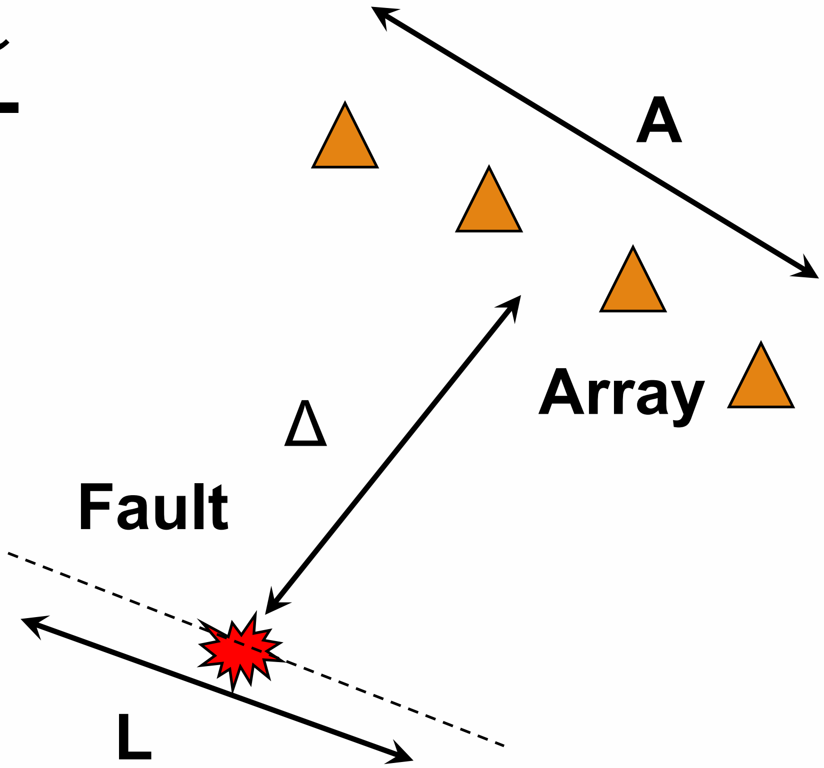

Point Spread Function

$$y(t) = \sum_k x_k(t + \tau_k(\theta))$$

$$B(\theta) = \int_t y(t)^2\, dt = \frac{1}{2\pi}\int_\omega |X(\omega)|^2 \left|\sum_k e^{i\omega\tau_k(\theta, r_k)}\right|^2 d\omega$$

$$A(\theta) = \left|\sum_k e^{i\omega\tau_n(\theta, r_k)}\right|^2$$

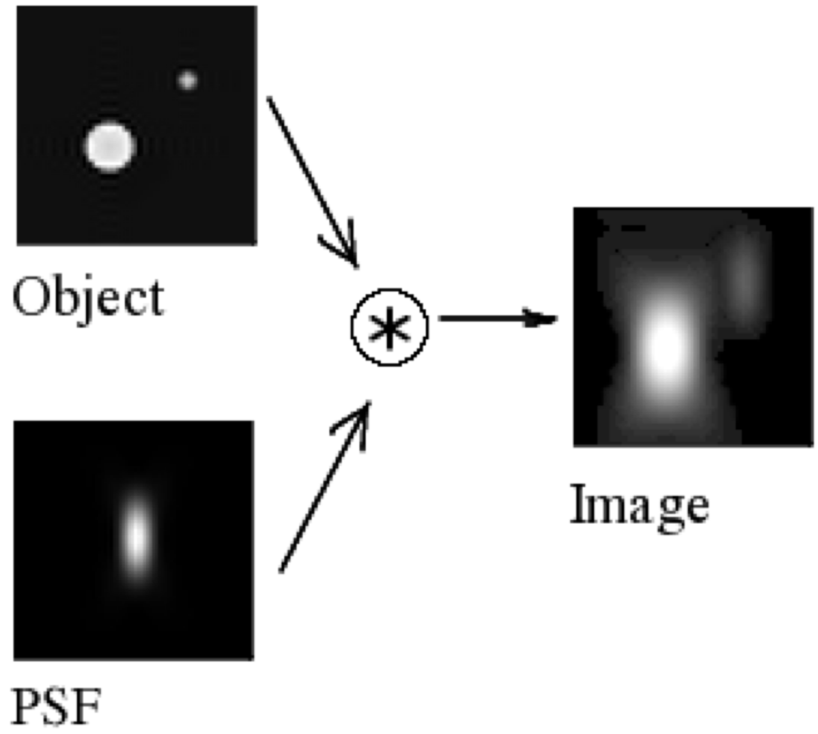

Point Spread Function

GRF array

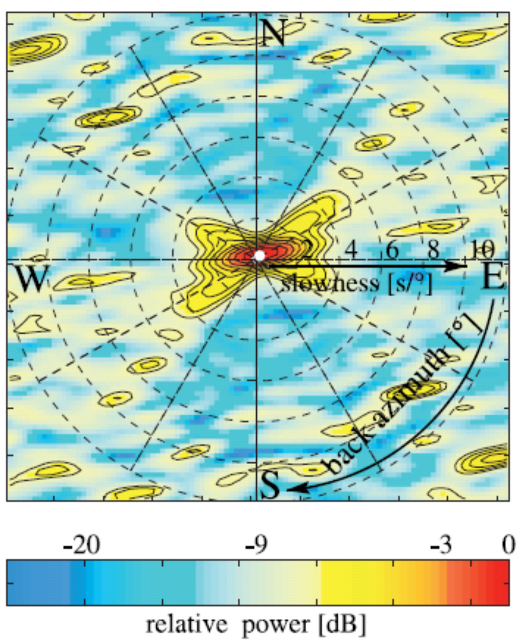

Yellow Knife Array

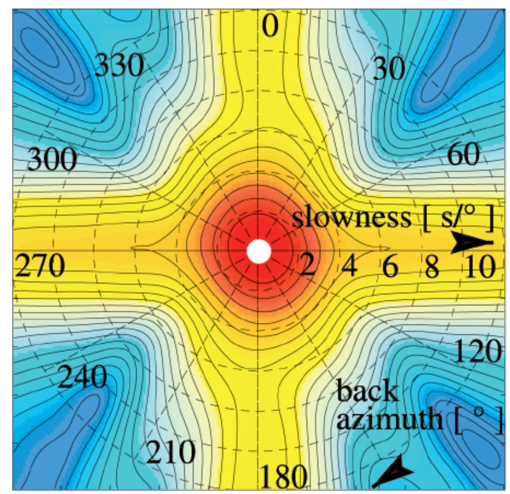

(Rost & Thomas ,2002)

Point Spreading Function of USArray

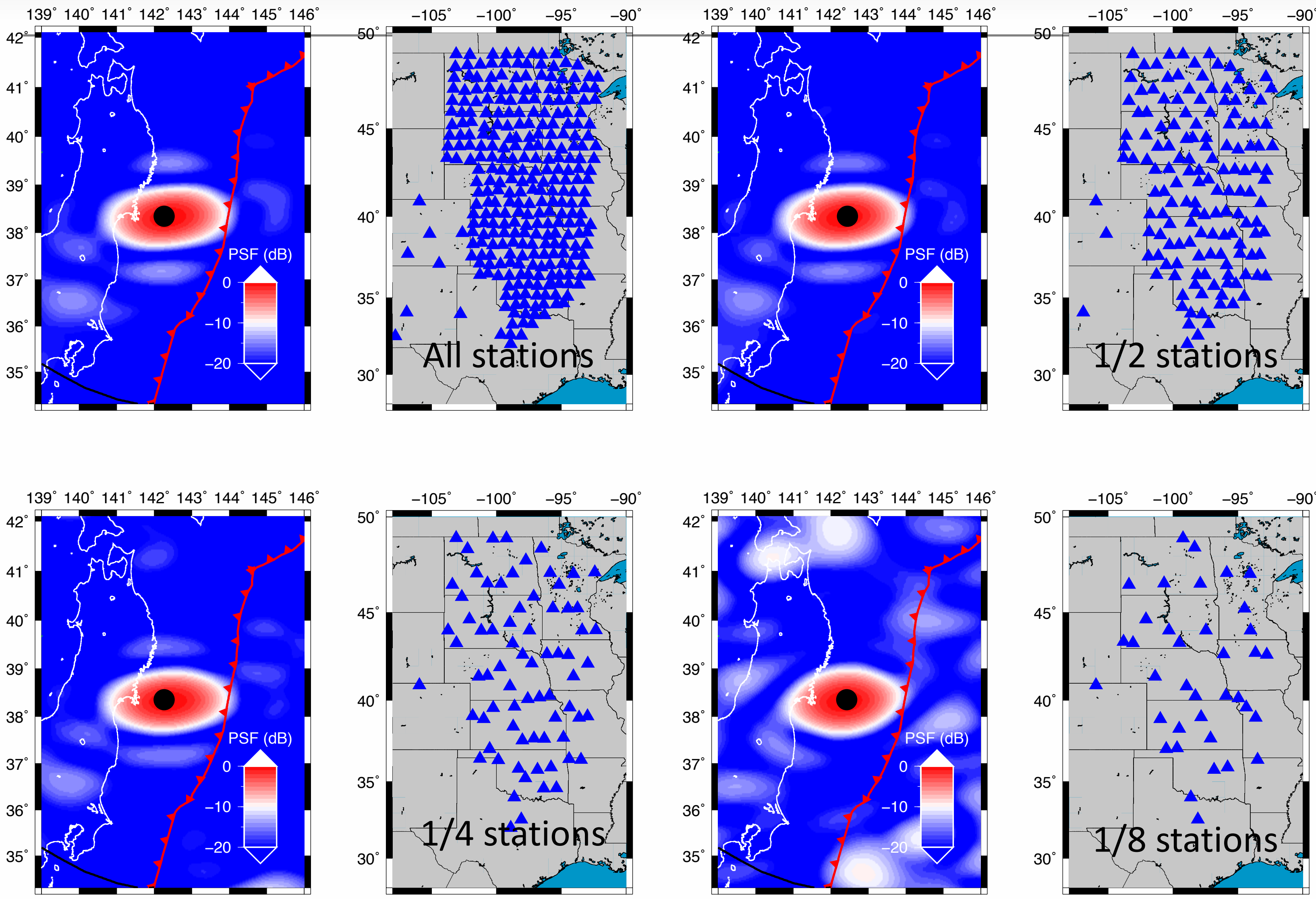

PSF of the TA backbone stations

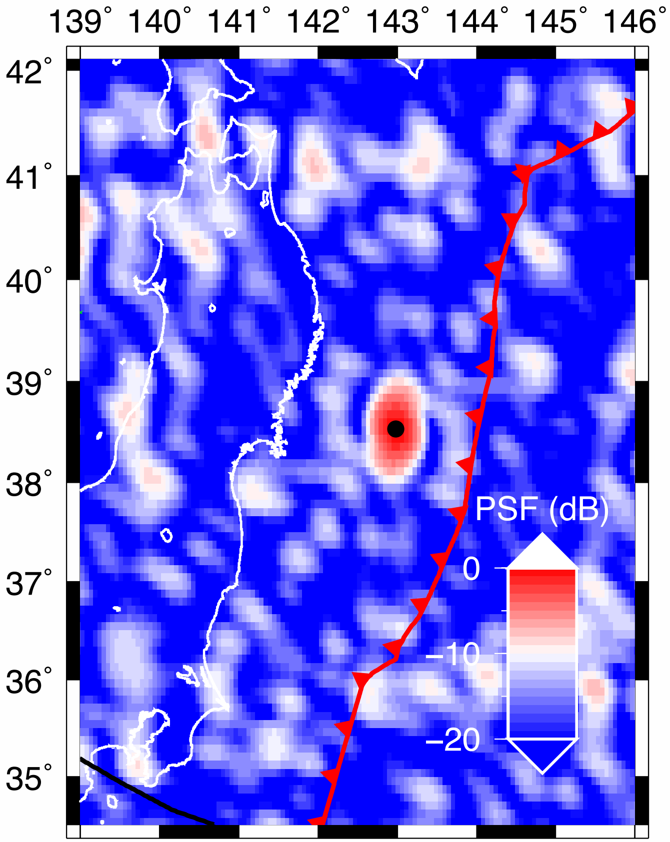

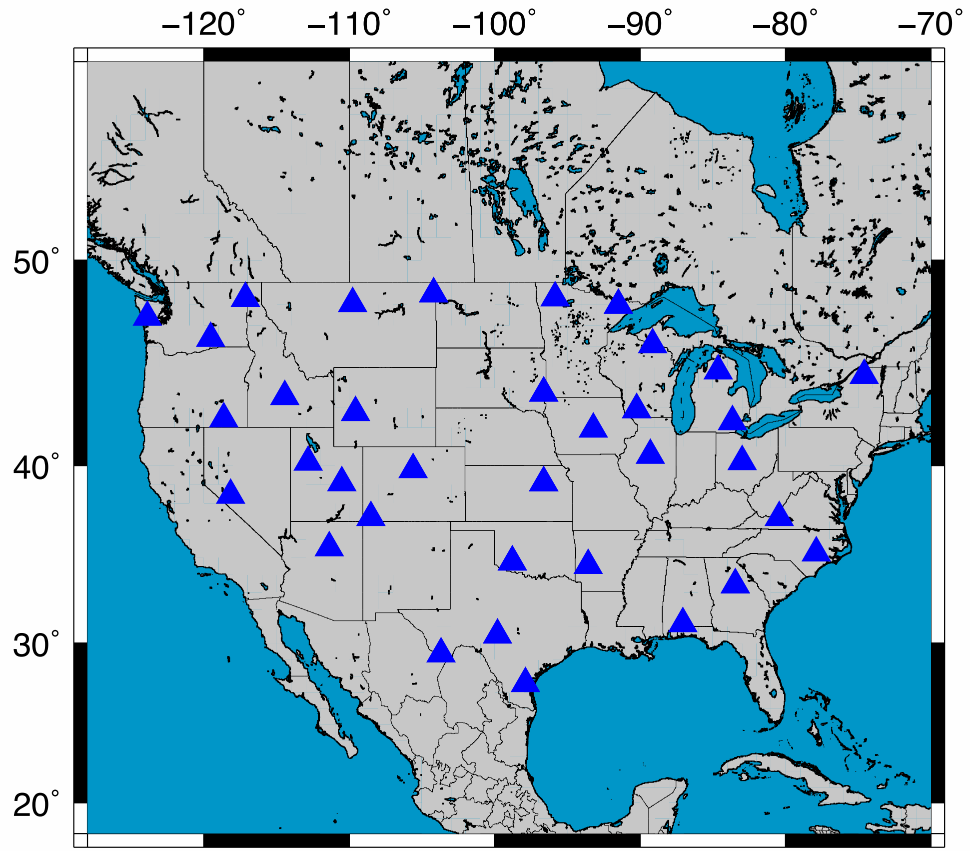

A Large Continental Array For Source Imaging

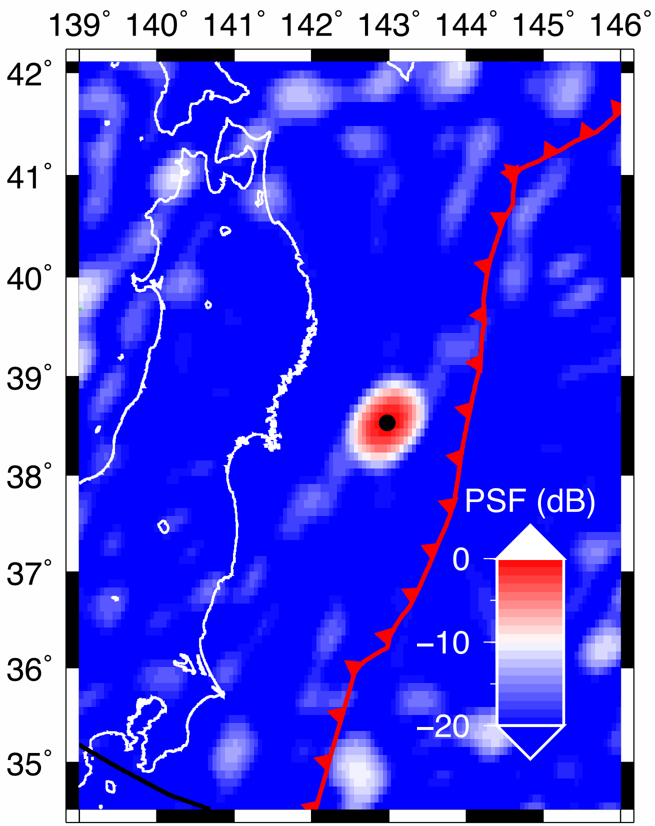

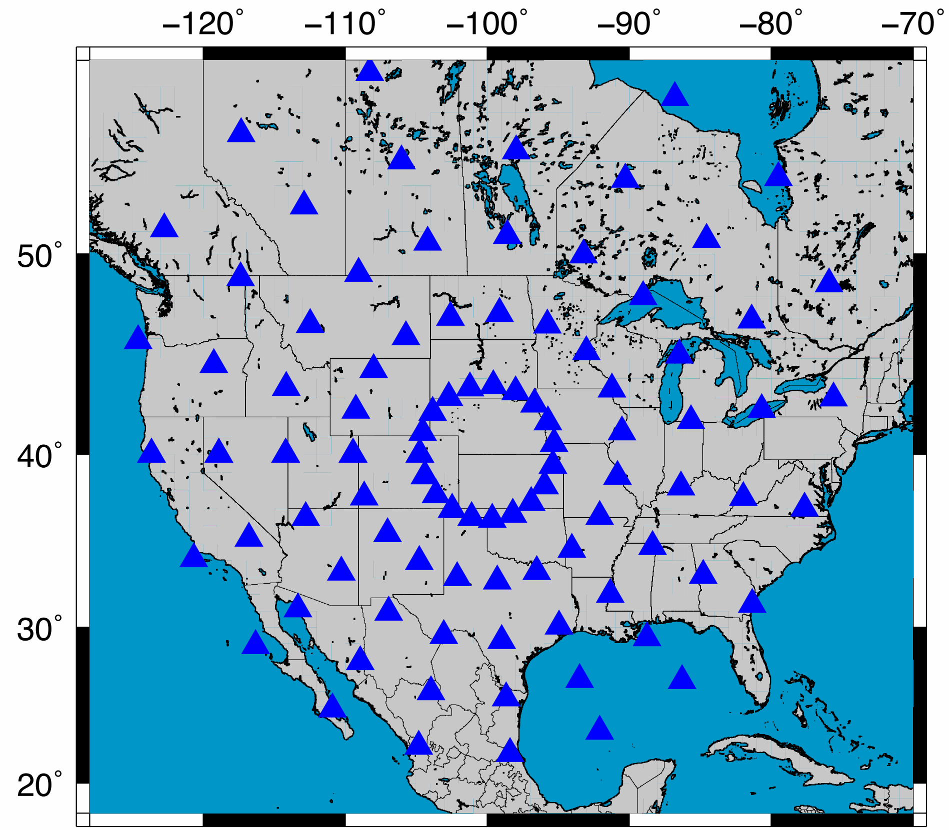

Multiple Signal Classification (MUSIC)

Significant development in the field of direction of arrivals

Seismic wave: transient, non-stationary, wideband , scattering, extended sources, not real-time, arbitrary geometry, less dense

Developed by Schmitz et al,1982

At least twice higher resolution than beamforming

Ability of separating closed spaced sources

Suitable for arbitrary array geometry

Combined with multi-taper cross spectrum estimation

Earthquake source study, small scale array, slowness diagram (Goldstein & Archuleta,1990)

Back-projections, large regional arrays (Meng et al., 2011)

Mathematical Signal Model

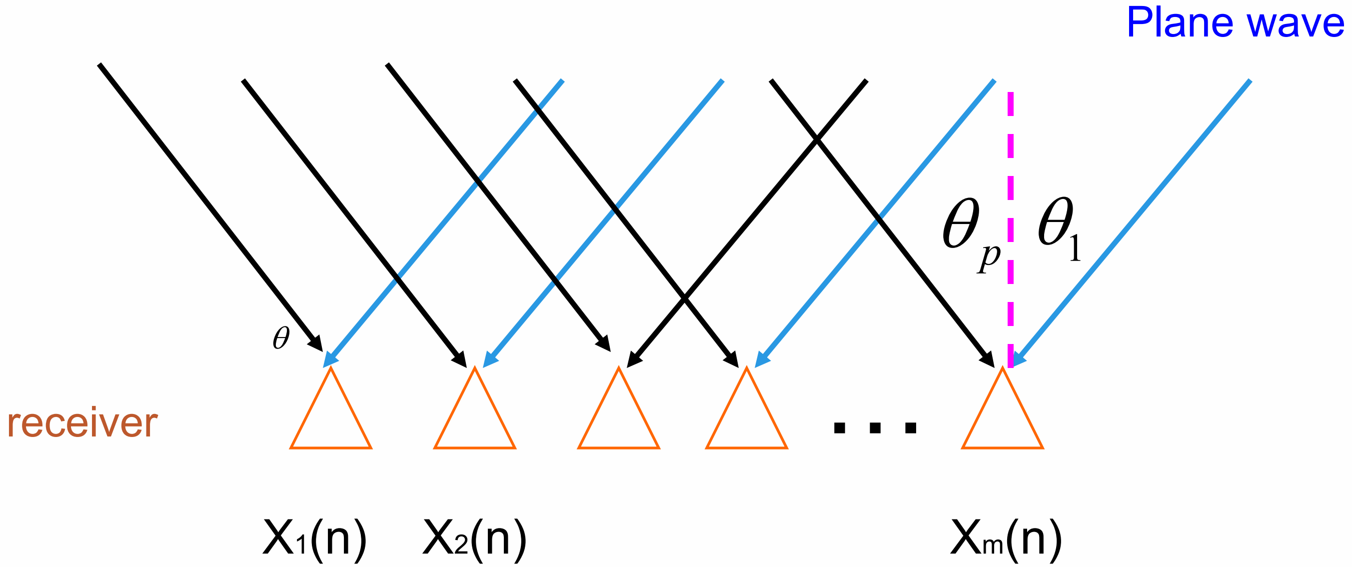

Signal model $$x_k(n) = \sum_{j=1}^{p} a_k(\theta_j) s_j(n) + e_k(n), k = 1, \ldots, m$$

Steering vector $$a_k = e^{i\omega\tau_k}$$

Signal $$s_j(n)$$

Gaussian white noise $$e_k(n)$$

Matrix form $$X(n) = A(\theta)S(n) + e(n)$$

Given X(n), solve for θ

Covariance matrix

$$\mathbf{R}_{xx} = E\left\{\mathbf{x}(n)\mathbf{x}^H(n)\right\}$$

Expectation of product between stations

$$= E\left\{\left[\mathbf{A}(\omega)\mathbf{s}(n)+\mathbf{e}(n)\right]\left[\mathbf{A}(\omega)\mathbf{s}(n)+\mathbf{e}(n)\right]^H\right\}$$

$$= \mathbf{A}(\omega)E\left\{\mathbf{s}(n)\mathbf{s}^H(n)\right\}\mathbf{A}^H(\omega) + \boxed{E\left\{\mathbf{e}(n)\mathbf{e}^H(n)\right\}}$$

$$= \mathbf{APA}^H + \sigma^2\mathbf{I}$$

Zero mean, same STD, independent

Eigenvalue decomposition

$$\mathbf{U}^H\mathbf{R}_{xx}\mathbf{U} = \mathbf{\Sigma}$$

$$\mathbf{U}^H\mathbf{APA}^H\mathbf{U} + \sigma^2\mathbf{I} = \mathbf{\Sigma}$$

Eigenvalues of Rxx

$$\lambda_i = \begin{cases} \alpha_{ii}^2 + \sigma^2, & i = 1, \quad , p \\ \sigma^2, & i = p+1, \quad , m \end{cases}$$

$$\begin{bmatrix} \alpha_{11}^2 & & & & & \\ & \ddots & & & & \\ & & \alpha_{pp}^2 & & & \\ & & & 0 & & \\ & & & & \ddots & \\ & & & & & 0 \end{bmatrix} + \sigma^2\mathbf{I}$$

$$\mathbf{U} = \left[\mathbf{S}\middle|\mathbf{G}\right] = [\mathbf{u}_1, \cdots, \mathbf{u}_n \mid \mathbf{u}_{n+1}, \cdots, \mathbf{u}_m]$$

Eigenvectors of Rxx

signal	noise
Subspace	Subspace
S (m×P)	G (m×(m-P))

Beamforming

$$P(\theta) = \left\| a(\theta)^H Rxx \right\| = a(\theta)^H RxxRxx^H a(\theta)^H$$

projection of signal steering vector on covariance matrix

$$P(\theta) = \frac{1}{\left\| a(\theta)^H G \right\|} = \frac{1}{a(\theta)^H G G^H a(\theta)^H}$$

MUSIC

1/(projection of signal steering vector on the noise space)

$$\theta_0 = \arg\max(P)$$

Signal location

Signal space is Orthogonal to noise space.

Resolution comparison

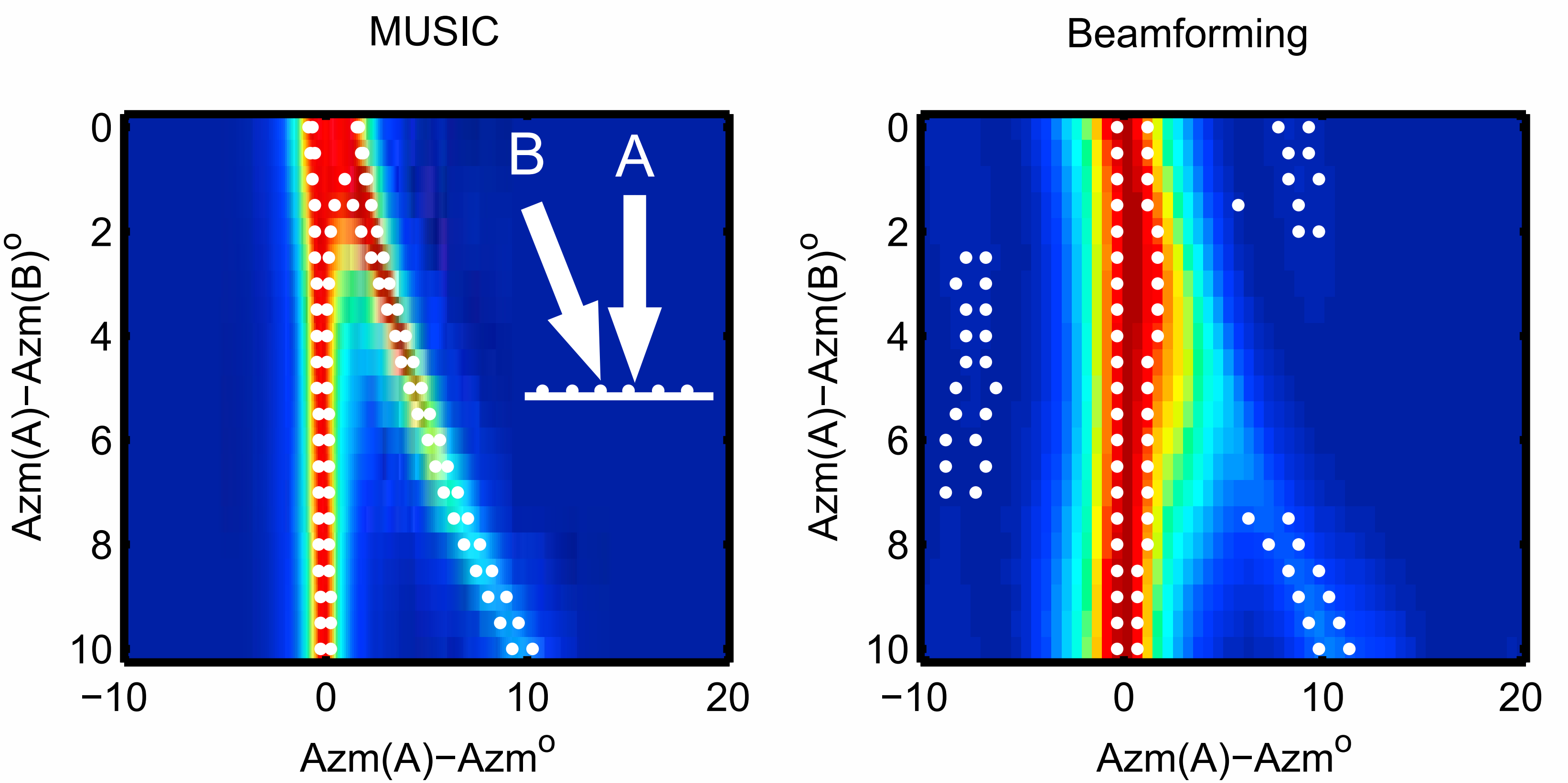

Synthetic test: separation of two plane waves by a linear array
MUSIC has higher resolution than beamforming

Meng et al, JGR (2012a)

2015 Mw 8.3 Illapel Earthquake

Ye et al., 2015

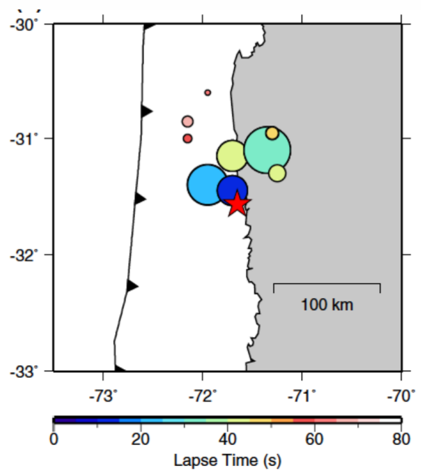

Fan et al., 2016

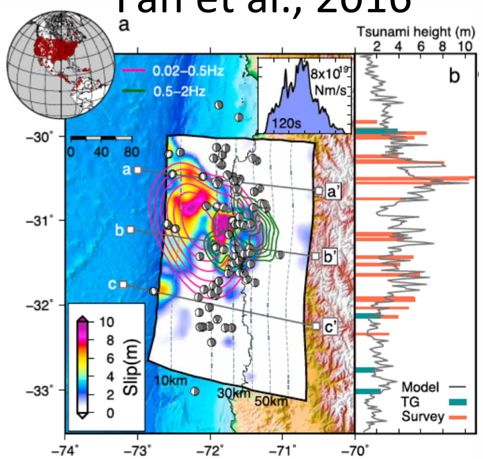

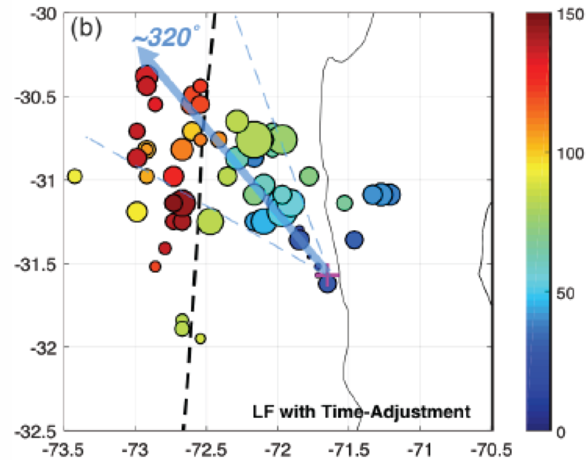

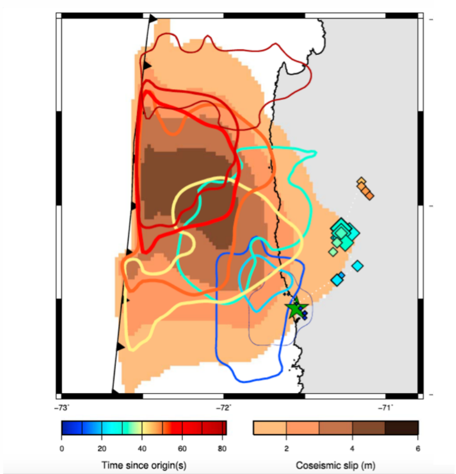

Tilman et al., 2015

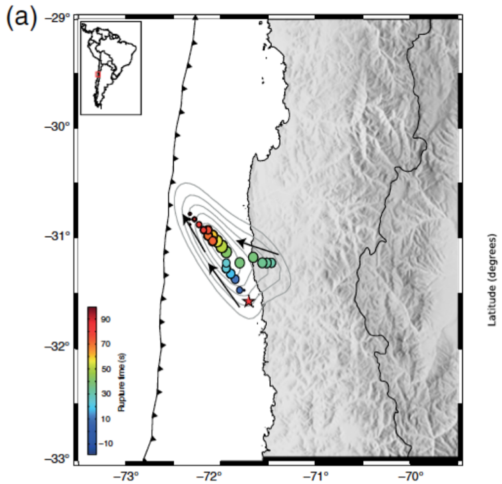

Ruiz et al., 2015

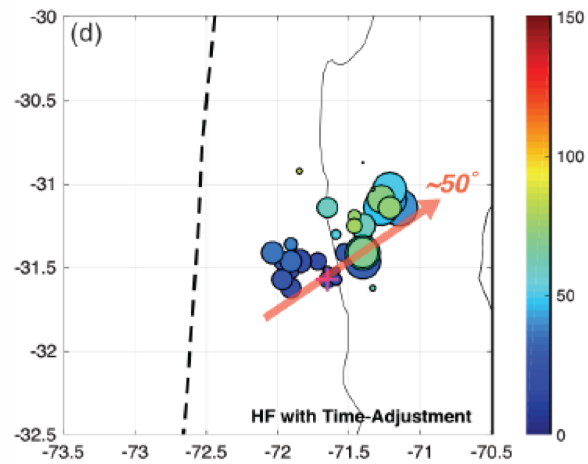

Yin and Denolle, 2017

Discrepancies of rupture extent in the along-dip direction

Rupture Front Splitting

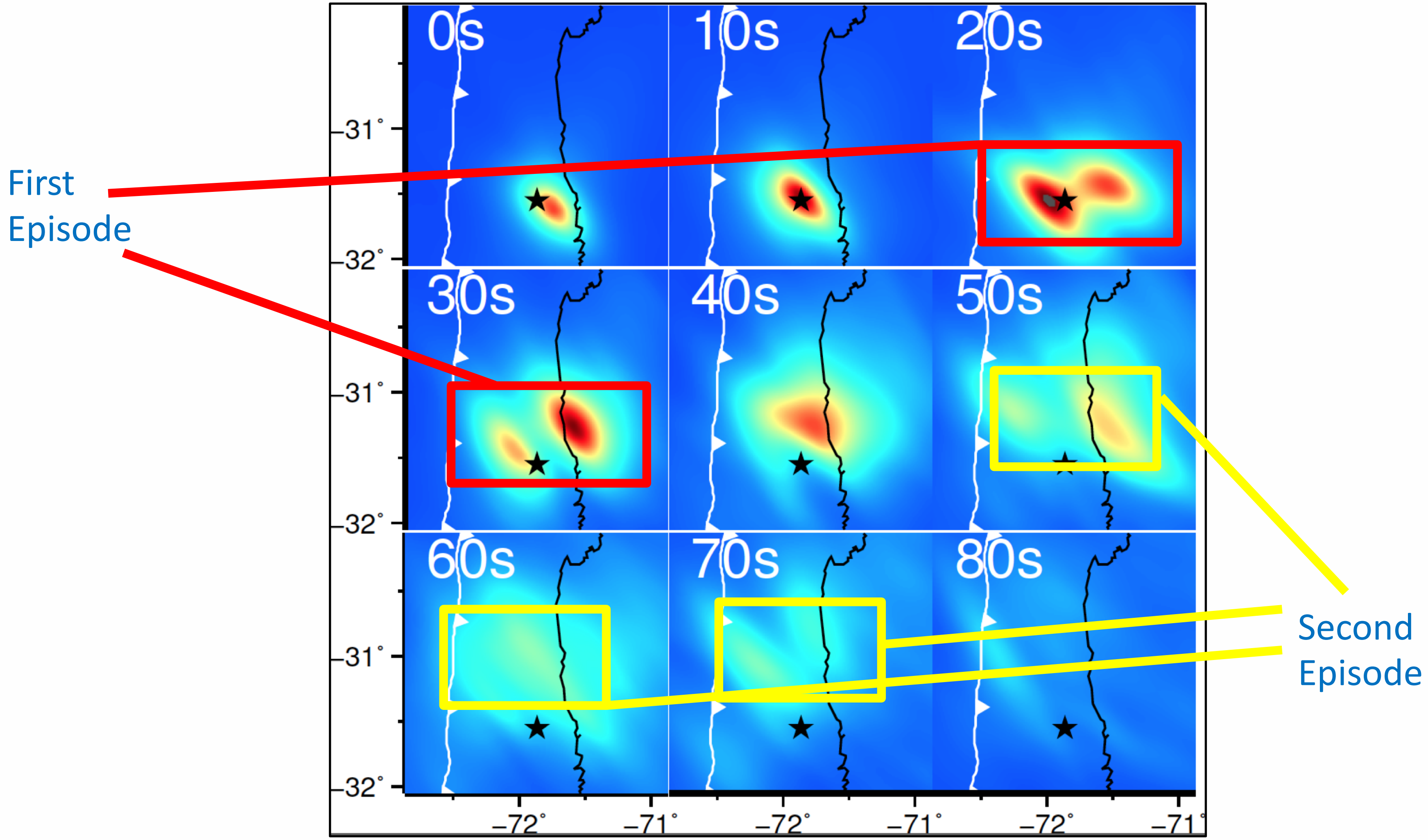

Meng et al., 2018

Two episodes of simultaneous high-frequency radiators

Encircling Rupture around Large Slip

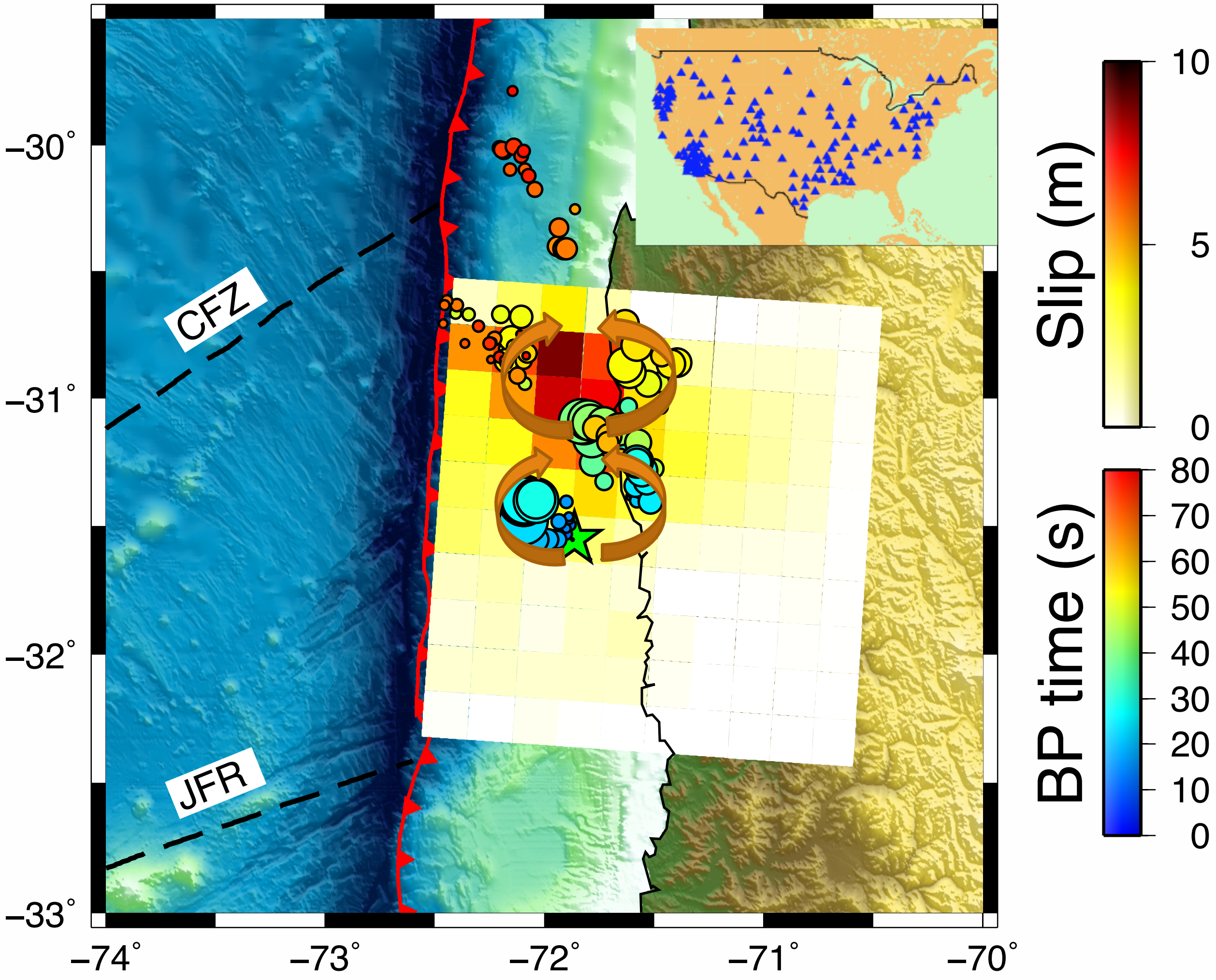

Validation by Strong-Motions

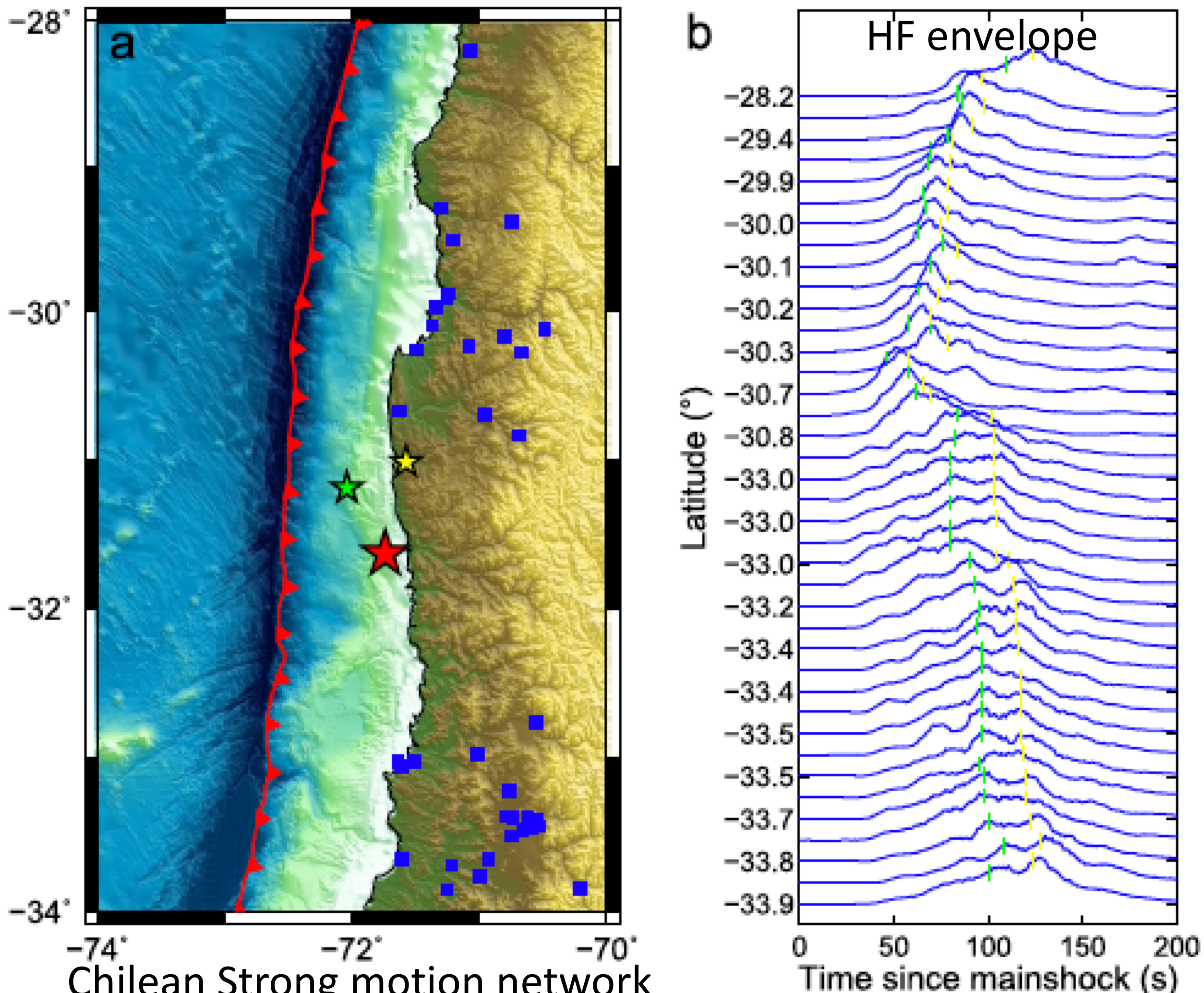

Chilean Strong motion network

The green star corresponds to the peak HF power in the up-dip branch.
The yellow star corresponds to the diverged rupture fronts reemerging as a single source.

2010 Mw 8.8 Maule Earthquake

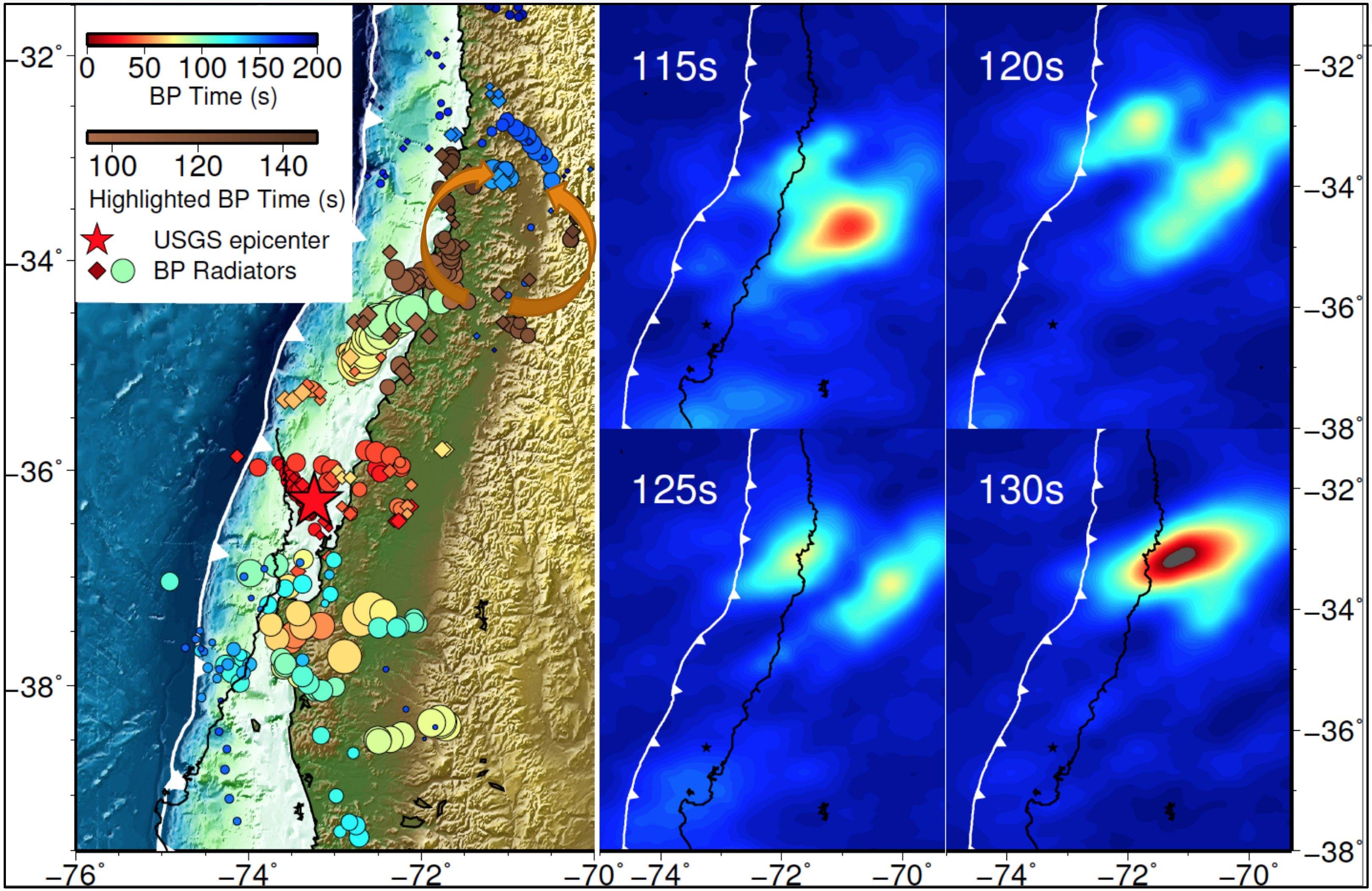

Military Analogy: Double Pincer Movement

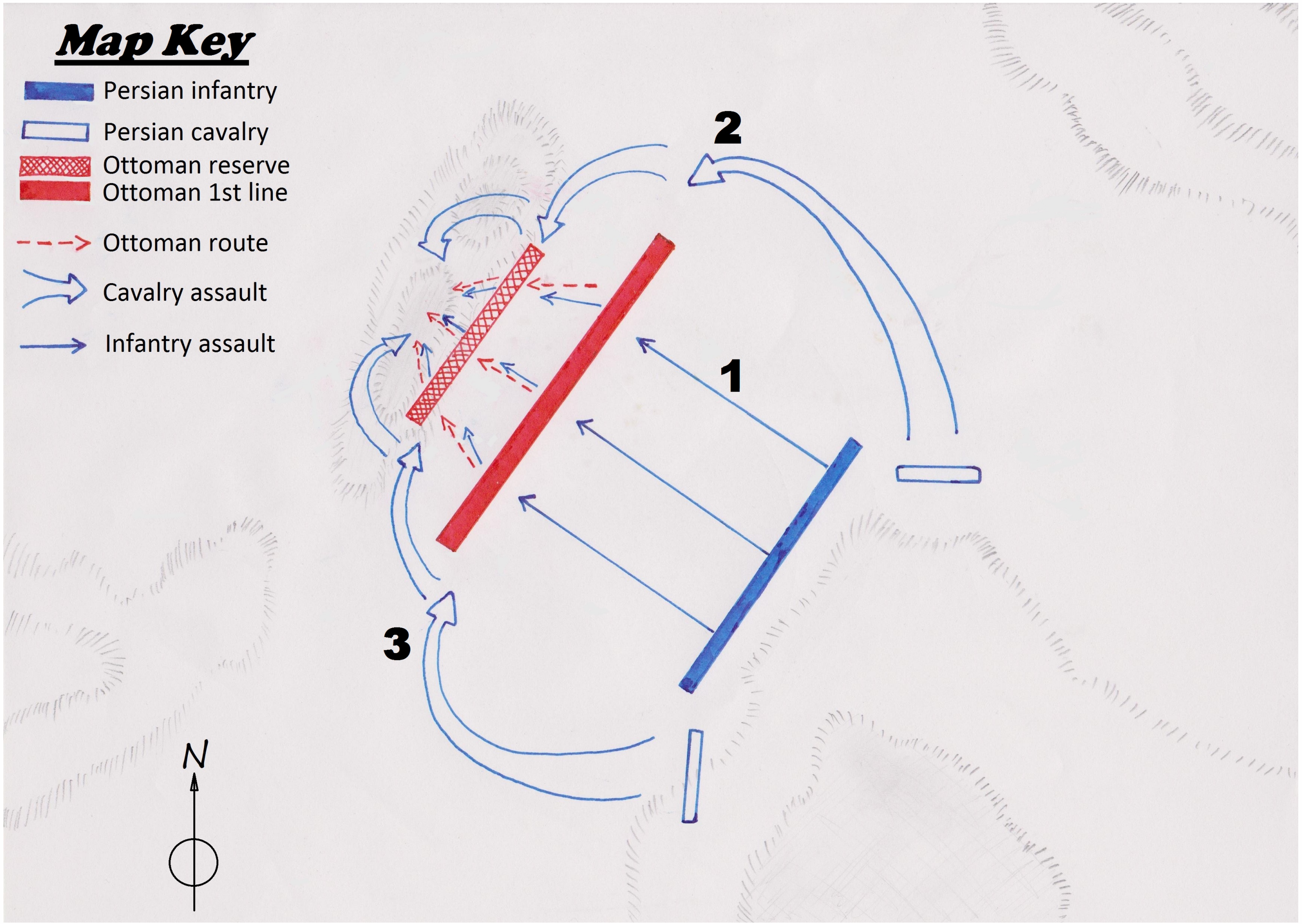

First proposed by Das and Kostrov, 1983; Credit: Pablo Ampuero

Rupture Encircling around a Single Asperity

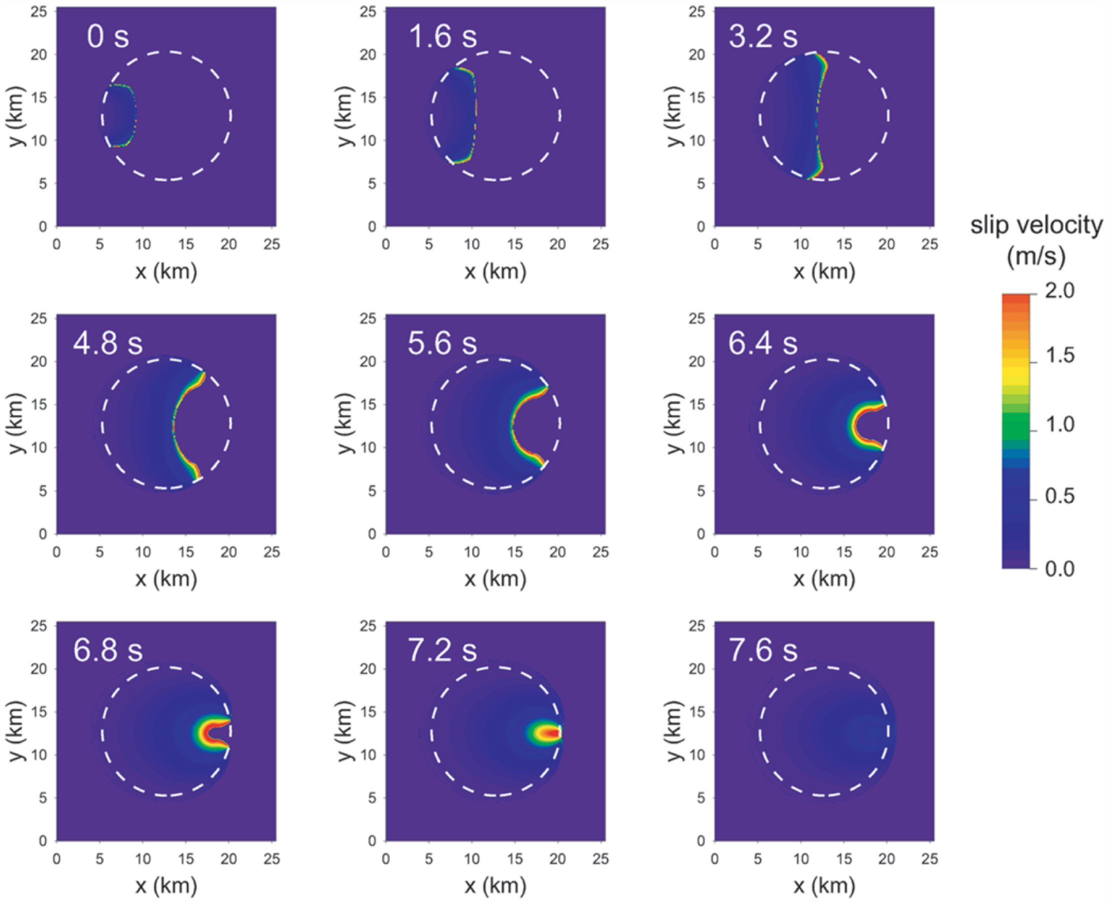

Kato, 2007

- Circular asperity embedded in creep
- Velocity weakening surrounded by velocity strengthening
- Stress concentration at the edge
- Delayed rupture in the asperity with larger slip
- Can be either asperity (large stress) or barrier (large strength)

Cascade-Up Model

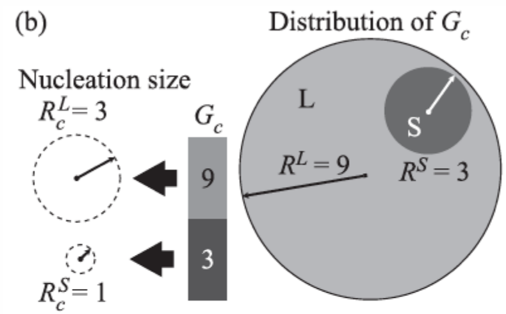

Noda et al., 2013

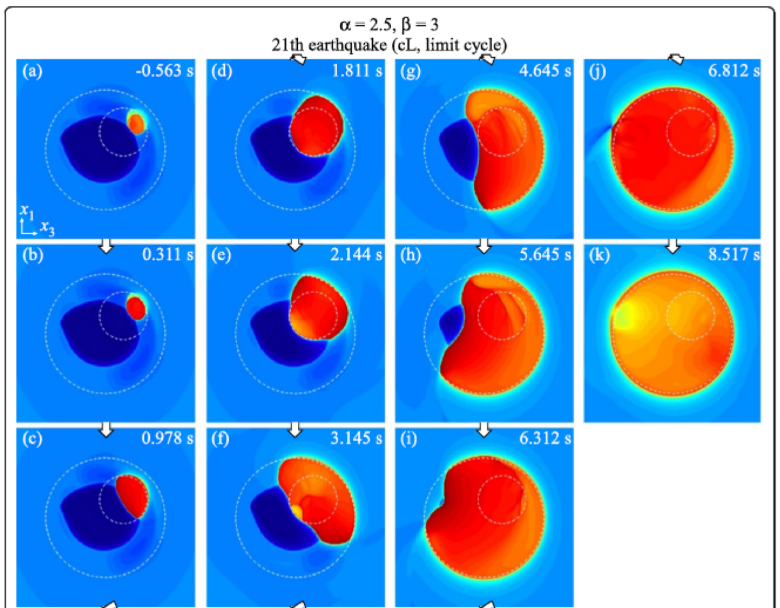

Figure 10 cL for $\alpha < \beta$. (a, b, c, d, e, f, g, h, i, j, k) Snapshots of the slip rate distribution during a typical cascade-up L event for $\alpha = 2.5$ and $\beta = 3$. The time after the moment acceleration exceeds threshold 10 PNm/s^2 is indicated in each panel. The color scale is the same as in Figure 3.

- Hierarchical asperity model or cascade-up growth model (Ide and Aochi, 2005; Hori and Miyazaki, 2011; Noda et al., 2013).
- Small fragile patches of smaller fracture energy embedded inside larger tough patches of large fracture energy
- The nucleation process initiates inside the small patch and tends to grow into large-scale rupture surrounding the rim of the large patch
- Between encircling front, the interior can either be locked and break later or slip simultaneously.
- In the latter case, the asperity might be too spatially smooth to generate HF radiations compared to the edge with heterogeneous stress concentrations

Noda et al., 2014

Slow Unlocking ahead of the Illapel Earthquake

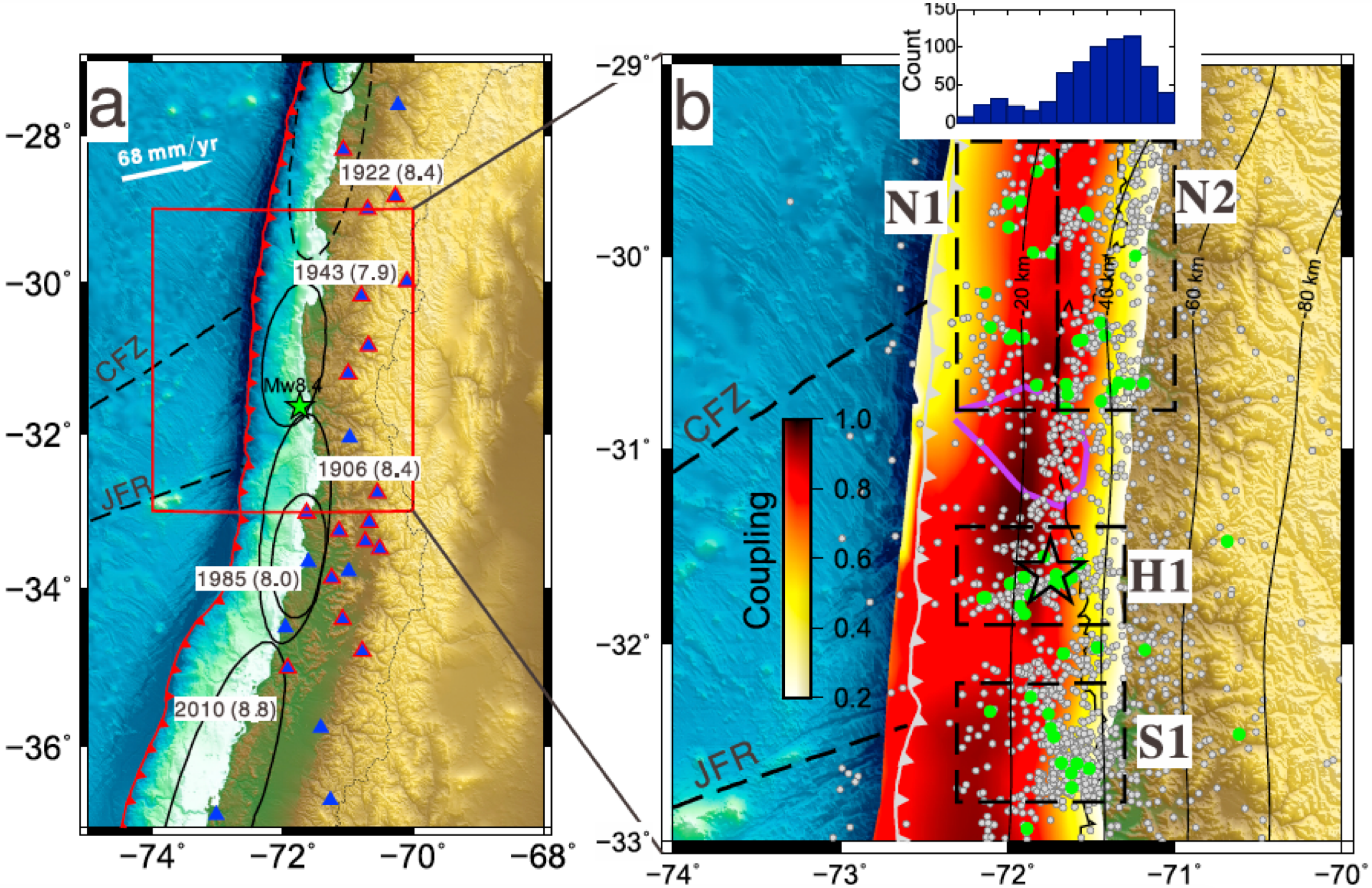

Cascade-up growth requires critical crack length (or fracture energy *Gc*) of larger slip patch reduced by creeping near the rim.

Slow unlocking of the illapel regions observed by repeating earthquakes and elevated seismicity (Huang and Meng., 2018).

Aseismic phenomena around the source region may cause reduction of fracture energy that would lead to dynamic cascade-up rupture.

Back-Projections Vs Repeaters

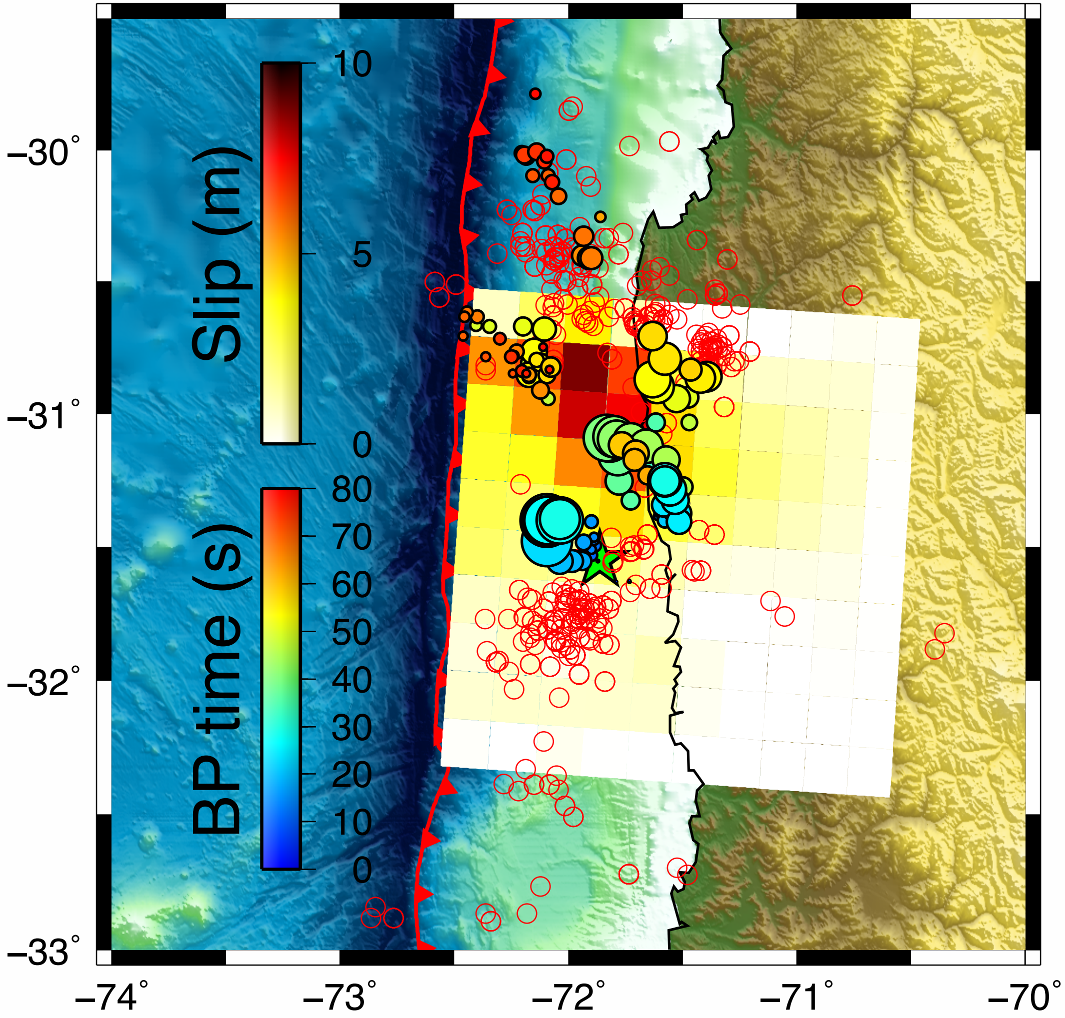

Red empty circles:
Post-seismic repeating earthquakes
Colored solid circles:
Co-seismic high-frequency radiators

Shared concept:
Brittle asperities surround by creep

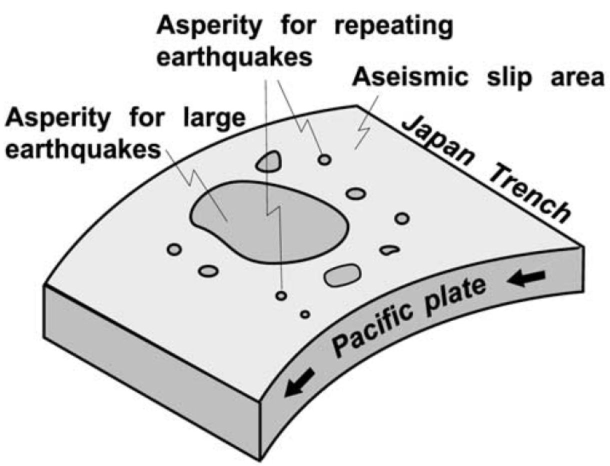

Uchida et al., 2003

Summary

- The high-resolution Multitaper-MUSIC BP is capable of separating closely spaced sources.
- The coseismic rupture is featured with two episode of simultaneous fronts seemingly unzipping the rim of a circular patch of large slip.
- Key features of the rupture process correlate with the prominent pulses recorded by local strong-motion network.
- The encircling rupture can be either explained by the asperity/barrier model or the cascade-up model.
- The cascade-up rupture is potentially linked to the aseismic phenomena observed rupture zone in the Illapel region.